

Genesis, Redox, and Acid–Base Relationships among W–C, W=C, and W≡C Functionalities over an Oxo Surface Modeled by Calix[4]arene

Luca Giannini,[†] Euro Solari,[†] Silvia Dovesi,[†] Carlo Floriani,^{*,†} Nazzareno Re,[‡] Angiola Chiesi-Villa,[§] and Corrado Rizzoli[§]

Contribution from the Institut de Chimie Minérale et Analytique, BCH, Université de Lausanne, CH-1015 Lausanne, Switzerland, Facoltà di Farmacia, Università degli Studi "G. D'Annunzio", I-66100 Chieti, Italy, and Dipartimento di Chimica, Università di Parma, I-43100 Parma, Italy

Received November 2, 1998

Abstract: This report deals with the chemistry of anionic W-alkylidynes generated over the oxo surface defined by a calix[4]arene tetraanion. The exhaustive alkylation of [*cis*-(Cl)₂W{*p*-Bu^t-calix[4]-(O)₄}] (1), with an excess of alkylating agent led to [{*p*-Bu^t-calix[4]-(O)₄}W≡C-R][M] (R = Ph, M = ¹/₂ Mg, 2; R = Prⁿ, M = Li, 3; R = SiMe₃, M = Li, 4). The protonation [PyHCl] of 2 and 3 led to the corresponding alkylidenes [{*p*-Bu^t-calix[4]-(O)₄}W=C(H)R] (R = Ph, 7; R = Prⁿ, 8), which were reversibly deprotonated back to the starting alkylidynes using LiBu. The reaction of 2–4 with AgNO₃ led to dimetallic alkylidenes [{*p*-Bu^t-calix[4]-(O)₄}W=C(R)Ag] (R = Ph, 12; R = Prⁿ, 13; R = SiMe₃, 14). The alkylation of 3 and 4 with MeOTf occurred at the carbon in 4 and at both carbon and oxygen in 3 leading to [{*p*-Bu^t-calix[4]-(O)₄}W=C(Me)-SiMe₃] (9) and to a mixture of [{*p*-Bu^t-calix[4]-(O)₄}W=C(Me)Prⁿ] (10) and [{*p*-Bu^t-calix[4]-(O)₃-(OMe)}W=C-Prⁿ] (11), respectively. The functionalization of the anionic alkylidynes was achieved by reacting 2 with electrophiles such as PhCHO leading to [{*p*-Bu^t-calix[4]-(O)₄}W=C(Ph)-C(H)(Ph)-O₂Mg(thf)] (15) and with Ph₂C=C=O forming [{*p*-Bu^t-calix[4]-(O)₄}W=C(Ph)-C(=CPh₂)-O₂Mg] (16). An indirect, but synthetically quite versatile, functionalization is the oxidation of 2 with I₂ producing [{*p*-Bu^t-calix[4]-(O)₄}-W=C(Ph)-I] (20). The alkylidenes 7 and 8 were unexpectedly unreactive in the presence of olefins and aldehydes, e.g., PhCHO, which formed a reversible adduct binding inside the calix[4]arene cavity. However, the trans labilization of the alkylidene functionality was achieved by reacting 7 with Bu^tNC, a reaction leading to *cis*-stilbene and the W=W dimer [{*μ*-*p*-Bu^t-calix[4]-(O)₄}]₂W₂(CNBu^t)₂ (18). The one-electron oxidation of 2 by Cp₂FeBPh₄ followed two different pathways via the common free-radical intermediate [{*p*-Bu^t-calix[4]-(O)₄}W=C•(Ph)], leading to either 7 (hydrogen abstraction) or [{*p*-Bu^t-calix[4]-(O)₄}]₂W₂(μ²-η²:η²-Ph₂C₂) (19). The nature of the anionic alkylidynes, the reaction pathways with electrophiles, and the one-electron oxidation reactions were analyzed using extended Hückel calculations.

Introduction

Our approach to metal–alkylidene¹ and metal–alkylidyne² chemistry is essentially focused on the attempt to make a bridge between homogeneous and heterogeneous systems³ using a preorganized quasi-planar tetraanionic O₄ set of oxygen donor atoms derived from the deprotonated form of calix[4]arene.⁴ To make this approach most significant we chose a metal, i.e., tungsten, which has played a major role in both heterogeneous and homogeneous systems since the discovery of the metathesis

reaction,⁵ and whose ligands of preference contain oxygen donor atoms.^{6,7} One might wonder what might be the consequence of using the calix[4]arene as ancillary ligand in metal–alkylidene and metal–alkylidyne chemistry. The metal bonded to the nearly planar calix[4]arene skeleton in its cone conformation displays three frontier orbitals, one σ and two π , particularly appropriate for stabilizing the M–C multiple bond functionality (see Extended Hückel Calculations); thus alkylidenes and alkylidynes may form spontaneously from conventional alkylation reactions. The other unique role of calix[4]arene, which makes comparisons with the heterogeneous metal–oxide systems⁸ valuable, is the basic surrounding of the metal where the oxygen donor

* To whom correspondence should be addressed.

[†] Institut de Chimie Minérale et Analytique.

[‡] Università degli Studi "G. D'Annunzio".

[§] Università di Parma.

(1) Feldman, J.; Schrock, R. R. *Prog. Inorg. Chem.* **1991**, 39, 1.

(2) Fischer, H.; Hofmann, P.; Kreissl, F. R.; Schrock, R. R.; Schubert, U.; Weiss, K. *Carbyne Complexes*; VCH: Weinheim, Germany, 1988.

(3) (a) Corker, J.; Lefebvre, F.; Lecuyer, C.; Dufaud, V.; Quignard, F.; Choplin, A.; Evans, J.; Basset, J.-M. *Science* **1996**, 271, 966. (b) Niccolai, G. P.; Basset, J.-M. *Appl. Catal., A* **1996**, 146, 145. (c) Vidal, V.; Theolier, A.; Thivolle-Cazat, J.; Basset, J.-M.; Corker, J. *J. Am. Chem. Soc.* **1996**, 118, 4595.

(4) (a) Gutsche, C. D. *Calixarenes*; The Royal Society of Chemistry: Cambridge, U.K., 1989. (b) *Calixarenes, A Versatile Class of Macrocyclic Compounds*; Vicens, J., Böhmer, V., Eds.; Kluwer: Dordrecht, The Netherlands, 1991.

(5) (a) Ivin, K. J.; Mol, J. C. *Olefin Metathesis and Metathesis Polymerization*, Academic: New York, 1997. (b) Moore, J. S. In *Comprehensive Organometallic Chemistry II*, Abel, E. W.; Stone, F. G. A.; Wilkinson, G., Eds.; Pergamon: Oxford, U.K., 1995; Vol. 12, Chapter 12.2.

(6) (a) Schrock, R. R. In *Reactions of Coordinated Ligands*; Braterman, P. S., Ed.; Plenum Press: New York, 1986; Vol. 1. (b) Schrock, R. R. *Acc. Chem. Res.* **1990**, 23, 158.

(7) Buhro, W. E.; Chisholm, M. H. *Adv. Organomet. Chem.* **1987**, 27, 311.

(8) (a) Srivastava, R. D. *Heterogeneous Catalytic Science*; CRC: Boca Raton, FL, 1988. (b) Gates, B. *Catalytic Chemistry*; Wiley: New York, 1992. (c) Bond, G. C. *Heterogeneous Catalysis, Principles and Applications*, 2nd ed.; Oxford University Press: New York, 1987.

atoms can assist the protonation–deprotonation of alkyldynes and, in general, their reaction with electrophiles. The so-called macrocyclic stabilization⁹ would help greatly in keeping the metal–calix[4]arene fragment resistant to protic acids and strong electrophiles. We should also mention that the use of a tetraanionic macrocycle would lead to anionic alkyldynes, thus providing the best entry to functionalized alkyldynes. Anionic alkyldynes would also allow one to set up a novel redox chemistry in the field.

This report covers the topics outlined above: (i) the genesis of W-anionic alkyldynes; (ii) their reversible protonation and deprotonation reactions; (iii) their metalation with carbophilic metals leading to dimetallic alkyldynes; (iv) their unusual transformation into functionalized alkyldynes using appropriate electrophiles such as aldehydes and ketenes; (v) their oxidative coupling to μ^2 - η^2 : η^2 -acetylene derivatives.

Experimental Section

All operations were carried out under an atmosphere of purified nitrogen. All solvents were purified by standard methods and freshly distilled prior to use. NMR spectra were recorded on 200-AC or DPX-400 Bruker instrument. IR spectra were recorded with a Perkin-Elmer FT 1600 spectrophotometer. GC analyses were carried out using a Hewlett-Packard 5890 series II gas chromatograph equipped with a TCD detector and a Carboxen 1006 capillary column. For H₂ detection, Ar was used instead of He as carrier gas. GC/MS analyses were carried out on a Hewlett-Packard 5890A gas chromatograph using a Petrocol DH capillary column coupled with an HP 5970 mass-selective detector. Li and Mg alkylating agents were either purchased (Fluka, Aldrich) or prepared by standard methods. Zn(CH₂Ph)₂ was prepared according to the literature.¹⁰ The synthesis of **1** has been performed as previously reported.¹¹ Photolyses were performed in a Solarbox (Cofomegra S.R.L.) equipped with a xenon lamp (540 W m⁻² at 340 nm), using standard laboratory glassware.

Synthesis of 2. Mg(CH₂Ph)₂ (52 mL, 1.22 N, 63.4 mmol) was added to a toluene (350 mL) suspension of **1**·2(C₇H₈) (23.0 g, 21.2 mmol) at –25 °C. The resulting red solution was allowed to warm to 0 °C overnight and then to room temperature. Toluene was evaporated and THF (500 mL) added to give an ochre mixture, which was stirred at room temperature for 2 days. Bright yellow **2**·6(C₄H₈O) was then collected, washed with THF (3 × 50 mL), and dried in vacuo (17.0 g, 59%). Anal. Calcd for C₇₅H₁₀₅Mg_{0.5}O₁₀W: C, 66.11; H, 7.77. Found: C, 65.80; H, 8.15. ¹H NMR (Py-*d*₅, 300 K, ppm): δ 7.27 (s, 8H, ArH), 7.10 (m, 2H, ArH), 7.03 (m, 2H, ArH), 6.65 (m, 1H, ArH), 5.26 (d, *J* = 11.6 Hz, 4H, *endo*-CH₂), 3.62 (m, 24H, THF), 3.33 (d, *J* = 11.6 Hz, 4H, *exo*-CH₂), 1.59 (m, 24H, THF), 1.22 (s, 36H, Bu^t). ¹³C NMR (Py-*d*₅, 300 K): δ 267.9 ppm. The X-ray analysis was carried out on the compound recrystallized from pyridine, [$\{[p\text{-Bu}^t\text{-calix}[4]-(\text{O})_4\text{-W}=\text{C}(\text{H})\text{Si}(\text{CH}_3)_3\} \cdot \frac{1}{2}\{\text{Mg}(\text{Py})_6\} \cdot 2\text{Py}$].

Synthesis of 3. LiBu (33 mL, 1.70 N, 56.1 mmol) was added to a toluene (250 mL) suspension of **1**·2(C₇H₈) (20.3 g, 18.9 mmol) at –30 °C, stirred overnight at that temperature, and then allowed to reach room temperature. THF (50 mL) was added, giving a suspension. Volatiles were removed in vacuo, and Et₂O (250 mL) was added to the residue. The mixture was filtered and, after the addition of DME (40 mL), taken to dryness. **3**·2(C₄H₁₀O₂)·0.5LiCl was collected from pentane (100 mL) and further washed with 50 mL of the same solvent (10.2 g, 49.4%). Anal. Calcd for C₅₆H₇₉Cl_{0.5}Li_{1.5}O₈W: C, 61.58; H, 7.29. Found: C, 61.54; H, 7.44. ¹H NMR (Py-*d*₅, 300 K): δ 7.15 (s, 8H, ArH), 5.20 (d, *J* = 11.6 Hz, 4H, *endo*-CH₂), 4.08 (t, *J* = 6.6 Hz, 2H, WCCH₂CH₂CH₃), 3.48 (s, 8H, DME), 3.25 (s, 12H, DME),

overlapping with 3.23 (d, *J* = 11.6 Hz, 4H, *exo*-CH₂), 1.80 (m, 2H, WCCH₂CH₂CH₃), 1.46 (t, *J* = 7.2 Hz, 3H, WCCH₂CH₂CH₃), 1.16 (s, 36H, Bu^t). ¹³C NMR (Py-*d*₅, 300 K): δ 276.6 (WC(Pr), *J*_{CW} = 278 Hz), 48.3 (WCCH₂CH₂CH₃), 27.0 (WCCH₂CH₂CH₃), 14.5 (WCCH₂-CH₂CH₃). Photolysis in DME of the deprotonated form of **5** leads to **3**·3(C₄H₁₀O₂), free of LiCl.¹²

Synthesis of 4. LiCH₂SiMe₃ (5.63 g, 60 mmol) was added to a suspension of **1**·2(C₇H₈) (21.7 g, 20.0 mmol) in toluene (250 mL) at –25 °C and allowed to warm to 0 °C overnight. After the addition of DME (30 mL), volatiles were removed in vacuo and Et₂O (600 mL) was added to the residue. LiCl was filtered off, and after further addition of DME (30 mL), the yellow solution was taken to dryness. Bright yellow **4**·2(C₄H₁₀O₂) was collected from pentane (100 mL), further washed with pentane (3 × 25 mL), and dried in vacuo (15.6 g, 71%). Anal. Calcd for C₅₆H₈₁LiO₈SiW: C, 61.08; H, 7.41. Found: C, 61.12; H, 7.86. ¹H NMR (Py-*d*₅, 300 K, ppm): δ 7.15 (s, 8H, ArH), 5.25 (d, *J* = 11.6 Hz, 4H, *endo*-CH₂), 3.47 (s, 8H, DME), 3.25 (s, 12H, DME), overlapping with, 3.26 (d, *J* = 11.6 Hz, 4H, *exo*-CH₂), 1.16 (s, 36H, Bu^t), 0.24 (s, 9H, SiMe₃). ¹³C NMR (Py-*d*₅, 300 K): δ 308.1 (WC(SiMe₃)). Crystals suitable for X-ray analysis were obtained from cooling THF/toluene solutions. When the reaction was performed by the addition of LiCH₂SiMe₃ (0.87 g, 9.2 mmol) to a suspension of **1**·2(C₇H₈) (3.3 g, 3.0 mmol) in frozen Et₂O (80 mL), which was then allowed to melt and then warm under stirring to room temperature in a closed Schlenk tube, no H₂ could be detected by GC analysis of the gas phase. NMR analysis of the yellow suspension showed clean **4**. Clean **4** was also obtained performing the reaction in THF at –30 °C.

Reacting **4**·2(C₄H₁₀O₂) (3.08 g, 2.80 mmol) with PyHCl (0.334 g, 2.89 mmol) in Et₂O at room temperature, [$\{[p\text{-Bu}^t\text{-calix}[4]-(\text{O})_4\text{-W}=\text{C}(\text{H})\text{Si}(\text{CH}_3)_3\} \cdot 2\text{PyHCl}$] was cleanly formed. ¹H NMR (C₆D₆, 300 K): δ 10.35 (s, 1H, WC(H)Si(CH₃)₃), 7.07 (s, 8H, ArH), 4.98 (d, *J* = 12.2 Hz, 4H, *endo*-CH₂), 3.26 (d, *J* = 12.2 Hz, 4H, *exo*-CH₂), 1.08 (s, 36H, Bu^t), 0.48 (s, 9H, W=C(H)SiMe₃). Due to its extreme solubility, this alkyldyne was not isolated. The reaction of [$\{[p\text{-Bu}^t\text{-calix}[4]-(\text{O})_4\text{-W}=\text{C}(\text{H})\text{Si}(\text{CH}_3)_3\} \cdot 2\text{PyHCl}$] with a stoichiometric amount of BuLi (in toluene at –30 °C) led to pure **4**, as determined by ¹H NMR spectroscopy.

Synthesis of 5. MgBr(CH₂)₄MgBr¹³ (15 mL, 0.365 M in THF, 5.47 mmol) was added to a suspension of **1**·2(C₇H₈) (5.70 g, 5.25 mmol) in toluene (150 mL) at –25 °C, to give a red solution, which was allowed to warm to room temperature overnight. Dioxane (1 mL) was added, volatiles were evaporated in vacuo, and the residue was extracted with Et₂O (150 mL) for 3 days. Solvent was evaporated and orange **5**·(C₄H₁₀O) was washed with pentane, collected, and dried in vacuo (2.25 g, 45%). Anal. Calcd for C₅₂H₇₀O₅W: C, 65.13; H, 7.36. Found: C, 64.84; H, 7.53. ¹H NMR (C₆D₆, 298 K, ppm): δ 7.15 (s, 8H, ArH), 4.47 (d, 4H, *J* = 13.2 Hz, *endo*-CH₂), 3.99 (m, 4H, C₄H₈), 3.60 (m, 4H, C₄H₈), 3.27 (d, 4H, *J* = 13.2 Hz, *exo*-CH₂), 1.28 (s, 36H, Bu^t).

Synthesis of 6. LiCH₂SiMe₃ (15 mL, 0.254 M in toluene, 3.81 mmol) was added to a suspension of **1**·2(C₇H₈) (4.13 g, 3.8 mmol) in THF (100 mL) at –10 °C. The mixture was stirred at 0 °C overnight, warmed to room temperature, and filtered. THF was evaporated in vacuo down to ~50 mL, Et₂O was added, and the mixture was allowed to stand overnight at –25 °C, to give **6**·3(C₄H₈O) as red needles which were collected and dried in vacuo (2.4 g, 56%). Anal. Calcd for C₅₆H₇₆Cl₂-LiO₇W: C, 59.90; H, 6.82. Found: C, 59.95; H, 6.78. ¹H NMR (CD₃-CN, 298 K, ppm): δ 12.2 (s, 4H), 5.50 (s, 4H), 3.69 (m, THF), overlapping with 3.67 (s), 1.86 (m, 12H, THF), 1.41 (s, 18H, Bu^t), 1.32 (s, 18H, Bu^t).

6·3(C₄H₈O) (1.19 g, 1.06 mmol) was reacted with LiCH₂SiMe₃ (8.4 mL, 0.254 M in toluene, 2.13 mmol) in toluene (50 mL) at –30 °C. After stirring at this temperature overnight and at room temperature for 2 h, a yellow suspension was obtained. ¹H NMR analysis revealed only a minor amount of **4** (20–30%), the main products gave signals spread over 30 ppm.

Synthesis of 7. Method A. Zn(CH₂Ph)₂ (3.16 g, 12.7 mmol) was added to a suspension of **1**·2(C₇H₈) (13.1 g, 12.1 mmol) in toluene (500 mL). The resulting mixture was stirred at room temperature over-

(9) (a) *Stereochemistry of Organometallic and Inorganic Compounds*. Volume 2: *Stereochemical and Stereophysical Behaviour of Macrocycles*; Bernal, I., Ed.; Elsevier: Amsterdam, 1987. (b) Dietrich, B.; Viout, P.; Lehn, J.-M. *Macrocyclic Chemistry*; VCH: Weinheim, 1993.

(10) Schrock, R. R. *J. Organomet. Chem.* **1976**, *122*, 209.

(11) (a) Corazza, F.; Floriani, C.; Chiesi-Villa, A.; Rizzoli, C. *Inorg. Chem.* **1991**, *30*, 4465. (b) Giannini, L.; Solari, E.; Floriani, C.; Re, N.; Chiesi-Villa, A.; Rizzoli, C. *Inorg. Chem.*, in press.

(12) Giannini, L.; Guillemot, G.; Solari, E.; Floriani, C.; Re, N.; Chiesi-Villa, A.; Rizzoli, C. *J. Am. Chem. Soc.* **1999**, *121*, 2797.

(13) (a) Sommer, L. H.; Anslu, G. R. *J. Am. Chem. Soc.* **1955**, *77*, 2482. (b) Azuma, Y.; Newcomb, M. *Organometallics* **1984**, *3*, 9.

night, at 50 °C for 2 h, and at 70 °C for 5 h. Buⁿ₄NCl (3.51 g, 12.6 mmol) was added, and the suspension was stirred for 2 h at 100 °C. A solid was filtered off the hot mixture, volatiles were evaporated, and pentane (300 mL) was added. The product was collected and dried in vacuo (7.37 g, 66%). Anal. Calcd for C₅₁H₅₈O₄W: C, 66.67; H, 6.36. Found: C, 66.65; H, 6.76.

Synthesis of 7. Method B. Cp₂FeBPh₄ (2.37 g, 4.69 mmol) was added to a suspension of 2·6(C₄H₈O) (5.81 g, 4.26 mmol) in Et₂O (230 mL) at -20 °C. The resultant mixture was stirred at this temperature overnight and then at room temperature to give a yellow-orange suspension. The solid was extracted overnight with its own mother liquors, volatiles were then evaporated to dryness, and pentane was (50 mL) added to the residue. The orange solid was collected and dried in vacuo (2.86 g, 73.1%). Anal. Calcd for C₅₁H₅₈O₄W: C, 66.67; H, 6.36. Found: C, 66.86; H, 6.63.

Synthesis of 7. Method C. PyHCl (0.665 g, 5.75 mmol) and 2·6(C₄H₈O) (7.55 g, 5.54 mmol) were stirred in Et₂O (200 mL) overnight to give a dark suspension. After an addition of toluene (70 mL), the mixture was taken to dryness and toluene (160 mL) was added to the residue. A white solid was filtered off, and volatiles were evaporated to give brown 7·(C₇H₈), which was washed with pentane (40 mL) and dried in vacuo (4.58 g, 82%). Anal. Calcd for C₅₈H₆₆O₄W: C, 68.91; H, 6.58. Found: C, 68.94; H, 6.76. ¹H NMR (CDCl₃, 298 K, ppm): δ 10.16 (s, 1H, WC(H)Ph), 7.63 (m, 2H, Ph), 7.21 (m, 2H, Ph), overlapping with, 7.20 (s, 8H, ArH), 6.90 (m, 1H, Ph), 4.70 (d, 4H, J = 12.2 Hz, *endo*-CH₂), 3.38 (d, 4H, J = 12.2 Hz, *exo*-CH₂), 2.40 (s, 3H, tol), 1.29 (s, 36H, Bu^t). ¹H NMR (Py-*d*₅, 300 K): δ 10.98 (s, 1H, WC(H)Ph), 7.52 (m, 4H, Ph), 7.33 (s, 8H, ArH), 6.82 (m, 1H, Ph), 5.08 (d, 4H, J = 12.2 Hz, *endo*-CH₂), 3.45 (d, 4H, J = 12.2 Hz, *exo*-CH₂), 2.20 (s, 3H, tol), 1.16 (s, 36H, Bu^t). ¹H NMR (C₆D₆, 300 K, ppm): δ 10.20 (s, 1H, WC(H)Ph), 7.30 (m, 2H, Ph), 7.17 (m, 2H, Ph), 7.08 (s, 8H, ArH), 6.55 (m, 1H, Ph), 4.99 (d, 4H, J = 12.2 Hz, *endo*-CH₂), 3.24 (d, 4H, J = 12.2 Hz, *exo*-CH₂), 2.10 (s, 3H, tol), 1.08 (s, 36H, Bu^t). ¹³C NMR (C₆D₆, 300 K): δ 260.5 (WC(Ph)H). Crystals suitable for X-ray analysis were obtained by extraction in Et₂O, using the methodology reported in ref 14.

Complex 7 was found to be exceedingly thermally (12 h, 80 °C) and photochemically stable. It was coordinated by PhCHO in toluene and C₆D₆ solutions. IR of a 1:1 mixture (tol, ν_{max} cm⁻¹): 1705.8 (m), 1683.4 (m), 1660 (m). ¹H NMR, excess PhCHO: 9.93 ppm W=C(H)-Ph (vs 10.20 ppm without added ligands), PhCHO very broad at 8.9 ppm (vs 9.67 ppm for free PhCHO). At room temperature, bright yellow [*p*-Bu^t-calix[4]-(O)₄]W=O became visible after 24 h. Solutions containing 7 and PhC(Me)O in a 1:1 ratio or in excess of the ketone showed NMR and IR spectra consisting of those of the two components superimposed.

Synthesis of 8. PyHCl (0.22 g, 1.9 mmol) was added to a solution of 3·2(C₄H₁₀O₂)·0.5LiCl (2.07 g, 1.9 mmol) in Et₂O (100 mL) and the mixture stirred for 2 h. A white solid was filtered off, volatiles were removed in vacuo, and pentane was added to the residue. 8 was then collected as a brown solid and dried in vacuo (0.97 g, 57%). Anal. Calcd for C₄₈H₆₀O₄W: C, 65.16; H, 6.84. Found: C, 64.85; H, 6.64. ¹H NMR (C₆D₆, 300 K): δ 10.0 (t, J = 7.5 Hz, 1H, WC(Pr)H), 7.07 (s, 8H, ArH), 5.47 (m, 2H, WCHCH₂CH₂CH₃), 4.95 (d, J = 12.2 Hz, 4H, *endo*-CH₂), 3.24 (d, J = 12.2 Hz, 4H, *exo*-CH₂), 1.69 (m, 2H, WCHCH₂CH₂CH₃), 1.15 (t, J = 7.2 Hz, 3H, WCCH₂CH₂CH₃), 1.08 (s, 36H, Bu^t). ¹H NMR (Py-*d*₅, 300 K): δ 10.7 (br d, 1H, W=C(H)-Pr), 7.33 (s, 8H, ArH), 5.63 (m, 2H, WCHCH₂CH₂CH₃), 4.90 (d, J = 12.2 Hz, 4H, *endo*-CH₂), 3.48 (d, J = 12.2 Hz, 4H, *exo*-CH₂), 1.88 (m, 2H, WCCH₂CH₂CH₃), 1.26 (m, 3H, WCCH₂CH₂CH₃), overlapping with 1.16 (s, 36H, Bu^t). ¹³C NMR (C₆D₆, 300 K): δ 272 (WC(Pr)H), J_{CW} = 180 Hz, J_{CH} = 142 Hz), 41.6 (WCCH₂CH₂CH₃), 29.5 (WCCH₂CH₂CH₃), 14.5 (WCCH₂CH₂CH₃).

The reaction of 8 with a stoichiometric amount of BuLi in toluene at -30 °C led to pure 3, as determined by ¹H NMR spectroscopy. 8 was found to be thermally (12 h, 60 °C) and photochemically very stable, and it was coordinated by PhCHO in solution. IR of a 1:1 mixture (tol, ν_{max} cm⁻¹): 1705.8 (m), 1683.8 (m), 1660.4 (m). 8 showed major shifts in ¹H NMR on addition of BuⁿNC; solutions containing excess

of the latter evolve to give M-M bonded dimer 18. Complex 8 was best obtained by photolysis of 5 in toluene.¹²

Synthesis of 9. MeOTf (0.24 g, 1.46 mmol) was added to a yellow suspension of 4·2(C₄H₁₀O₂) (1.60 g, 1.46 mmol) in toluene (120 mL) and stirred overnight to give an orange mixture. Solids were filtered off, volatiles were evaporated, and pentane (40 mL) was added. The resulting solution was kept at 5 °C for 5 days to give ochre crystals of 9. The product was then collected and dried in vacuo (0.63 g, 45.3%). ¹H NMR (CD₂Cl₂, 298 K): δ 7.08 (s, 8H, ArH), 5.64 (s, 3H, Me), 4.58 (d, 4H, J = 12.7 Hz, *endo*-CH₂), 3.26 (d, 4H, J = 12.7 Hz, *exo*-CH₂), 1.18 (s, 36H, Bu^t), 0.50 (s, 9H, SiMe₃). ¹³C NMR (CDCl₃, 298 K): δ 276 (WC(Me)SiMe₃), J_{CW} = 166.5 Hz.

Synthesis of 10 and 11. MeOTf (0.25 g, 1.52 mmol) was added to a suspension of 3·3(C₄H₁₀O₂) (1.76 g, 1.51 mmol) in toluene (120 mL) and stirred overnight. A white solid was filtered off, volatiles were evaporated, and pentane (40 mL) was added. The resulting solution was kept at 5 °C for 5 days to give a solid, which was collected and dried in vacuo (0.83 g), containing 10 and 11 in roughly equal amounts.

For 10: ¹H NMR (C₆D₆, 300 K, ppm): 7.07 (s, 8H, ArH), 5.41 (s, 3H, W=C(Me)Pr), 5.17 (t, 2H, J = 6.85 Hz, WC(CH₃)CH₂CH₂CH₃), 4.93 (d, 4H, *endo*-CH₂), 3.24 (d, 4H, *exo*-CH₂), 1.73 (m, 2H, WC(CH₃)CH₂CH₂CH₃), 1.27 (t, 3H, WC(CH₃)CH₂CH₂CH₃), 1.09 (s, 36H, Bu^t). ¹H NMR (CDCl₃, 300 K, ppm): 7.13 (s, 8H, ArH), 5.52 (s, 3H, WC(Pr)Me), 5.17 (t, 2H, J = 7.3 Hz, WC(Me)CH₂CH₂CH₃), 4.57 (d, 4H, J = 12.2 Hz, *endo*-CH₂), 3.27 (d, 4H, J = 12.2 Hz, *exo*-CH₂), 1.84 (m, 2H, WC(Me)CH₂CH₂CH₃), 1.28-1.16 overlapping (36H, Bu^t, 3H, WC(Me)CH₂CH₂CH₃). ¹³C NMR (CDCl₃, 300 K, ppm): δ 28.4 (WC(Me)Pr), 46.4 (WC(Me)CH₂CH₂CH₃), 293.0 (WC(Me)Pr), J_{CW} = 177 Hz).

For 11: ¹H NMR (C₆D₆, 300 K, ppm): δ 7.23 (d, 2H, J = 2.45 Hz, ArH), 7.21 (d, 2H, J = 2.45 Hz, ArH), 6.91 (s, 2H, ArH), 6.85 (s, 2H, ArH), 4.51 (s, 3H, OMe), from 4.97 to 4.91 (t, 2H, WCCH₂CH₂CH₃) overlapping with (d, 2H, *endo*-CH₂), 4.53 (d, 2H, *endo*-CH₂), 3.24 (d, 4H, *exo*-CH₂), 1.79 (m, 2H, WCCH₂CH₂CH₃), 1.40 (s, 18H, Bu^t), 1.09 (t, 3H, WCCH₂CH₂CH₃), 0.81 (s, 9H, Bu^t), 0.72 (s, 9H, Bu^t). ¹H NMR (CDCl₃, 300 K, ppm): δ 7.06 (s, 2H, ArH), 7.05 (d, 2H, J = 2.45 Hz, ArH), 7.02 (s, 2H, ArH), 7.00 (d, 2H, J = 2.45 Hz, ArH), 5.12 (s, 3H, OMe), 4.93 (t, 2H, J = 6.8 Hz, WCCH₂CH₂CH₃), 4.48 (d, 2H, J = 12.7 Hz, *endo*-CH₂), 4.42 (d, 2H, J = 12.7 Hz, *endo*-CH₂), 3.35 (d, 2H, J = 12.7 Hz, *exo*-CH₂), 3.18 (d, 2H, J = 12.7 Hz, *exo*-CH₂), 1.84 (m, 2H, WCCH₂CH₂CH₃), 1.28-1.16 overlapping (36H, Bu^t, 3H, WCCH₂CH₂CH₃). ¹³C NMR (CDCl₃, 300 K, ppm): δ 301.7 (WCCH₂CH₂CH₃), J_{CW} = 278 Hz), 80.7 (OCH₃), 49.3 (WCCH₂CH₂CH₃).

Synthesis of 12. AgNO₃ (0.70 g, 4.1 mmol) and 2·6(C₄H₈O) (5.58 g, 4.1 mmol) were suspended in THF (150 mL) and the mixture was stirred overnight, giving a suspension of a gray solid in a red supernatant. Volatiles were removed, and pentane (150 mL) was added. A pale solid was filtered off; the pentane solution was concentrated to 50 mL and kept at -25 °C for 4 days. Deep red 12 was collected from the cold mother liquors and dried in vacuo (2.4 g, 57%). Anal. Calcd for C₅₁H₅₇AgO₄W: C, 59.72; H, 5.60. Found: C, 59.95; H, 5.91. ¹H NMR (Py-*d*₅, 300 K): δ 7.50 (m, 2H, Ph), 7.27 (s, 8H, ArH), overlapping with 7.2 (m, 2H, Ph), 6.74 (m, 1H, Ph), 5.26 (d, J = 11.6 Hz, 4H, *endo*-CH₂), 3.36 (d, J = 11.6 Hz, 4H, *exo*-CH₂), 1.19 (s, 36H, Bu^t). ¹³C NMR (Py-*d*₅, 298 K): δ 265.6 (WC(Ph)), J_{CW} = 256 Hz). ¹H NMR (C₆D₆, 298 K, ppm): δ 8.12 (m, 2H, Ph), 7.11 (m, 2H, Ph), 6.94 (s, 8H, ArH), 6.81 (m, 1H, Ph), 4.83 (d, 4H, J = 12.7 Hz, *endo*-CH₂), 2.95 (d, 4H, J = 12.7 Hz, *exo*-CH₂), 1.10 (s, 36H, Bu^t). ¹³C NMR (C₆D₆, 298 K): δ 241.1 ({WC(Ph)}{μ-Ag}), J_{CAG} = 58 Hz). ¹H NMR (CD₂Cl₂, 298 K): δ 7.49 (m, 2H, Ph), 6.97 (s, 8H, ArH), 6.80 (m, 2H, Ph), 6.61 (m, 1H, Ph), 4.42 (d, 4H, J = 12.5 Hz, *endo*-CH₂), 2.88 (d, 4H, J = 12.5 Hz, *exo*-CH₂), 1.20 (s, 36H, Bu^t). ¹³C NMR (CD₂Cl₂, 298 K): δ 240.9 ({WC(Ph)}{μ-Ag}), J_{CAG} = 60 Hz).

Synthesis of 13. AgNO₃ (0.3 g, 1.77 mmol) was added to a solution of 3·3(C₄H₁₀O₂) (1.97 g, 1.70 mmol) in THF (100 mL) and the mixture stirred overnight. Volatiles were removed in vacuo, and the residue was extracted with Et₂O (100 mL). The resulting deep red solution was kept at -25 °C for 24 h to yield 13 as red needles (0.5 g, 30%). Anal. Calcd for C₄₈H₅₉AgO₄W: C, 58.14; H, 6.00. Found: C, 57.95; H, 6.03. ¹H NMR (Py-*d*₅, 300 K): δ 7.25 (s, 8H, ArH), 5.31 (d, J = 11.6 Hz, 4H, *endo*-CH₂), 4.74 (t, J = 6.8 Hz, 2H, WCCH₂CH₂CH₃),

3.35 (d, $J = 11.6$ Hz, 4H, *exo*-CH₂), 2.0 (m, 2H, WCCH₂CH₂CH₃), 1.41 (t, 3H, $J = 7.4$ Hz, WCCH₂CH₂CH₃), 1.19 (s, 36H, Bu^t). ¹³C NMR (Py-*d*₅, 300 K): δ 272 (W=C(Pr))₂{Ag}, 50.0 (WCCH₂CH₂CH₃), 27.9 (WCCH₂CH₂CH₃), 14.6 (WCCH₂CH₂CH₃). The X-ray analysis was performed on the solid recrystallized from pyridine/DME to give [{*p*-Bu^t-calix[4]-(O)₄}]₂W=C(Pr)₂{ μ -Ag(Py)}₂ (**13py**).

Synthesis of 14. AgNO₃ (0.50 g, 2.95 mmol) was added to a solution of 4·2(C₄H₁₀O₂) (3.03 g, 2.75 mmol) in THF (150 mL) and the mixture stirred overnight. Volatiles were removed in vacuo, and the residue was extracted with Et₂O (100 mL) over 6 h. **14** was collected at room temperature from the Et₂O mother liquors as an orange powder (1.5 g, 53%). Anal. Calcd for C₄₈H₆₁AgO₄SiW: C, 56.42; H, 6.01. Found: C, 56.10, H, 6.18. ¹H NMR (Py-*d*₅, 300 K): δ 7.23 (s, 8H, ArH), 5.07 (d, $J = 11.6$ Hz, 4H, *endo*-CH₂), 3.31 (d, $J = 11.6$ Hz, 4H, *exo*-CH₂), 1.16 (s, 36H, Bu^t), 0.56 (s, 9H, SiMe₃).

Synthesis of 15. PhCHO (0.18 g, 1.7 mmol) was added to a suspension of 2·6(C₄H₈O) (2.3 g, 1.7 mmol) in THF (100 mL), and the mixture was stirred for 1 h to give a blue solution. Volatiles were removed in vacuo, toluene was added to the residue, and the solution was filtered. Volatiles were evaporated again, and the residue was washed with pentane to give blue **15**·(C₅H₁₂), which was collected and dried in vacuo (1.3 g, 69%). Anal. Calcd for C₁₂₅H₁₄₆MgO₁₁W₂: C, 67.74; H, 6.64. Found: C, 67.66; H, 6.48. ¹H NMR (Py-*d*₅, 300 K): δ 10.67 (s, 2H, PhC(O)H), 7.9–6.4 (m, ArH), 5.96 (d, 2H, $J = 12.4$ Hz, *endo*-CH₂), 5.13 (d, 2H, $J = 13.0$ Hz, *endo*-CH₂), 4.79 (d, 2H, $J = 11.6$ Hz, *endo*-CH₂), 4.60 (d, 2H, $J = 12.6$ Hz, *endo*-CH₂), 4.14 (d, 2H, $J = 12.4$ Hz, *exo*-CH₂), 3.73 (d, 2H, $J = 13.0$ Hz, *exo*-CH₂), 3.63 (m, 4H, THF), 3.37 (m, 4H, *exo*-CH₂), 1.59 (m, 4H, THF), 1.54 (s, 18H, Bu^t), 1.45 (s, 18H, Bu^t), 1.2 (m, 6H, pentane), 0.98 (s, 18H, Bu^t), 0.79 (m, 6H, pentane), 0.74 (s, 18H, Bu^t). ¹H NMR (CD₂Cl₂, 300 K): δ 10.2 (s, 2H, PhC(O)H), 7.5–6.9 (m, 30H, ArH), 6.49 (m, 2H, ArH), 6.18 (m, 4H, ArH), 5.18 (d, 2H, $J = 12.5$ Hz, *endo*-CH₂), 4.69 (d, 2H, $J = 13.1$ Hz, *endo*-CH₂), 4.53 (d, 2H, $J = 11.5$ Hz, *endo*-CH₂), 3.87 (d, 2H, $J = 13.0$ Hz, *endo*-CH₂), 3.78 (m, 4H, thf), 3.53 (d, 2H, $J = 12.5$ Hz, *exo*-CH₂), 3.47 (d, 2H, $J = 13.1$ Hz, *exo*-CH₂), 3.33 (d, 2H, $J = 11.5$ Hz, *exo*-CH₂), 2.94 (d, 2H, $J = 13.0$ Hz, *exo*-CH₂), 2.61 (m, 4H, thf), 1.4 (m, 6H, pentane), 1.35 (s, 18H, Bu^t), 1.33 (s, 18H, Bu^t), 1.25 (s, 18H, Bu^t), 1.17 (s, 18H, Bu^t), 0.90 (m, 6H, pentane). ¹³C NMR (CD₂Cl₂, 298 K): δ 288 (W=C), 79.3 (W=C(Ph)C(Ph)(O)H).

Synthesis of 16. Diphenylketene (0.25 g, 1.29 mmol) and 2·6(C₄H₈O) (1.71 g, 1.25 mmol) were mixed in toluene (80 mL) to give a dark green solution. Volatiles were evaporated, pentane was added to the residue, and green **16**·2(C₇H₈) was collected and dried in vacuo (0.97 g, 64%). Anal. Calcd for C₁₄₄H₁₅₀O₁₀W₂Mg: C, 71.10; H, 6.22. Found: C, 71.21; H, 6.21. ¹H NMR (Py-*d*₅, 253 K): δ 7.8–6.4 (m, ArH), 5.45 (d, 4H, $J = 13.2$ Hz, *endo*-CH₂), 5.26 (d, 4H, $J = 11.7$ Hz, *endo*-CH₂), 3.57 (d, 4H, $J = 13.2$ Hz, *exo*-CH₂), 3.26 (d, 4H, $J = 11.7$ Hz, *exo*-CH₂), 2.11 (s, 6H, tol), 1.40 (s, 18H, Bu^t), 1.39 (s, 18H, Bu^t), 0.69 (s, 36H, Bu^t). Crystals suitable for X-ray analysis were obtained by cooling solutions in toluene/hexane at –25 °C.

Synthesis of 17. **7** (3.0 g, 3.26 mmol) and Bu^tNC (0.26 g, 3.1 mmol) were dissolved in toluene (120 mL). Volatiles were removed in vacuo, and pentane (70 mL) was added to the residue, which was then collected and dried in vacuo to give **17**·(C₅H₁₂) (2.0 g, 60%). Anal. Calcd for C₆₁H₇₉NO₄W: C, 68.21; H, 7.41; N, 1.30. Found: C, 67.83, H, 7.59, N, 1.04. ¹H NMR (tol-*d*₈, 300 K, ppm): δ 8.9 (br d, WC(H)Ph), 7.42 (br d, 2H, Ph), 7.17 (m, 2H, Ph), 7.13 (s, 8H, ArH), 6.50 (br d, 1H, Ph), 4.97 (br d, 4H, *endo*-CH₂), 3.29 (d, 4H, *exo*-CH₂), 1.2 (m, 6H, pentane), overlapping with 1.20 (s, 36H, Bu^t), 0.90 (m, 6H, pentane), –0.12 (br d, Bu^tNC). A sharp spectrum was obtained by lowering the temperature. ¹H NMR (tol-*d*₈, 260 K, ppm): δ 9.04 (s, 1H, WC(H)Ph), 7.46 (m, 2H, Ph), 7.21 (m, 2H, Ph), 7.12 (s, 8H, ArH), 6.48 (m, 1H, Ph), 5.14 (d, 4H, $J = 12.7$ Hz, *endo*-CH₂), 3.30 (d, 4H, $J = 12.7$ Hz, *exo*-CH₂), 1.27 (s, 36H, Bu^t), –0.21 (s, 9H, Bu^tNC). By adding an excess of Bu^tNC to the NMR sample, a sharp spectrum (except for coordinated Bu^tNC) was also obtained at room temperature. ¹H NMR (tol-*d*₈, 298 K, ppm): δ 8.90 (s, 1H, WC(H)Ph), 7.45 (m, 2H, Ph), 7.17 (m, 2H, Ph), 7.13 (s, 8H, ArH), 6.46 (m, 1H, Ph), 5.07 (d, 4H, $J = 12.7$ Hz, *endo*-CH₂), 3.30 (d, 4H, $J = 12.7$ Hz, *exo*-CH₂), 1.25 (s, 36H, Bu^t), 0.95 (excess Bu^tNC), –0.08 (br d, Bu^tNC). IR (toluene,

ν_{\max} cm^{–1}): 2194.7 (s), 2132.5 (m). Solutions of **17** evolved to give **18**. The reaction was faster when an excess of Bu^tNC was present.

Synthesis of 18. **8** (1.07 g, 1.21 mmol) and Bu^tNC (0.13 g, 1.56 mmol) were dissolved in toluene (80 mL). After 2 days, dark microcrystalline **18**·2(C₇H₈) had formed on the side of the flask and was collected and dried (0.45 g, 37%). The same product was obtained (with a longer reaction time) from the reaction of **7** and Bu^tNC in toluene. In the latter case, *cis*-stilbene (but no *trans*-stilbene) was detected by gas chromatography in the reaction mixture. Anal. Calcd for C₁₁₂H₁₃₈N₂O₈W₂: C, 66.99; H, 6.93; N, 1.40. Found: C, 66.83; H, 7.02; N, 1.23. ¹H NMR (CDCl₃, 298 K, ppm): δ 7.3–7.08 (m, 26H, ArH, tol), 4.90 (d, 4H, $J = 12.7$ Hz, *endo*-CH₂), 4.63 (d, 4H, $J = 12.2$ Hz, *endo*-CH₂), 3.42 (d, 4H, *exo*-CH₂), overlapping with 3.33 (d, 4H, *exo*-CH₂), 2.40 (s, 6H, tol), 1.31 (s, 18H, Bu^t), 1.25 (s, 36H, Bu^t), 1.23 (s, 18H, Bu^t), –0.03 (s, 18H, Bu^tNC). IR (Nujol, ν_{\max} cm^{–1}): 2202.8 (s). Crystals suitable for X-ray structural determination were obtained by performing the reaction between **7** and excess Bu^tNC in an NMR tube in C₆D₆.

Synthesis of 19. Cp₂FeBPh₄ (1.75 g, 3.46 mmol) and 2·6(C₄H₈O) (4.39 g, 3.22 mmol) were stirred in Et₂O at 0 °C overnight to give a red suspension. The solid was extracted overnight with its own mother liquors, and then volatiles were removed in vacuo. Pentane (50 mL) was added to the residue, and the resulting solution was allowed to stand overnight, yielding **19**·2(C₅H₁₂) as a microcrystalline red solid, which was collected and dried in vacuo (1.1 g, 33%). Anal. Calcd for C₁₁₂H₁₃₈O₈W₂: C, 67.94; H, 7.02. Found: C, 67.95; H, 7.29. ¹H NMR (C₆D₆, 298 K, ppm): δ 8.63 (m, 4H, Ph), 7.43 (m, 4H, Ph), 6.94 (s, 18H, ArH, Ph), 4.70 (d, 8H, $J = 12.4$ Hz, *endo*-CH₂), 3.04 (d, 8H, $J = 12.4$ Hz, *exo*-CH₂), 1.22 (m, 12H, pentane), 1.02 (s, 72H, Bu^t), 0.88 (m, 12H, pentane). ¹³C NMR (C₆D₆, 300 K): δ 207 (μ -C₅Ph₂). Crystals suitable for X-ray analysis were grown from hexane/benzene solutions at room temperature.

Synthesis of 20. I₂ (0.51 g, 2.0 mmol) was added to a yellow suspension of 2·6(C₄H₈O) (2.59 g, 1.90 mmol) in THF (120 mL) and stirred overnight at room temperature. The resulting mixture was filtered, volatiles were evaporated, and toluene (120 mL) was added, and the mixture was stirred overnight. The solution was filtered, volatiles were evaporated in vacuo, and pentane (40 mL) was added. Brown **20**·0.5(C₅H₁₂) was collected and dried in vacuo (1.25 g, 61%). Anal. Calcd for C₅₃H₆₃IO₄W: C, 59.45; H, 5.87. Found: C, 59.33; H, 5.85. ¹H NMR (CDCl₃, 300 K, ppm): δ 7.63 (m, 2H, ArH), 7.56 (m, 2H, ArH), 7.23 (s, 8H, ArH), 6.97 (m, 1H, ArH), 4.64 (d, 4H, $J = 12.7$ Hz, *endo*-CH₂), 3.29 (d, 4H, $J = 12.7$ Hz, *exo*-CH₂), 1.18 (s, 39H, Bu^t, pent), 0.86 (m, 3H, C₅H₁₂). ¹³C NMR (CDCl₃, 400 MHz, 300 K, ppm): δ 230.0 (W=C(I)Ph, $J_{\text{CW}} = 212$ Hz.). Crystals suitable for X-ray analysis were grown from a solution of toluene/heptane.

X-ray Crystallography for Complexes 2, 4, 7, 9, 13py, 16, and 19. Single crystals suitable for X-ray diffraction were grown from common organic solvents (Table 1). Data for **2**, **4**, and **13py** were collected on a Rigaku AFC6S diffractometer, for **7** and **16** on a Mar345 image plate detector diffractometer, for **9** on a Kuma CCD diffractometer, and for **19** on a Stoe IPDS diffractometer using Mo K α radiation. The solutions and refinements were carried out using the programs SHELX76¹⁵ and SHELX93.¹⁶ The details of the X-ray data collection, structure solution, and refinement are given in Supporting Information.¹⁷

Results

The Alkylation of [cis-(Cl)₂W]{*p*-Bu^t-calix[4]-(O)₄}. The first attempts to obtain alkyl derivatives of **1 by reaction with 1 or 2 equiv of Li and Mg alkylating agents did not lead to the expected products (see below). On the other hand, when a 3:1 molar ratio was used, alkyldiene derivatives **2–4** were readily obtained (Scheme 1). The reaction went well also when β -hydrogens were present, as in the case of **3**. The reaction solvents played an important role both in the selection of the**

(15) Sheldrick, G. M. SHELX76. Program for crystal structure determination. University of Cambridge; Cambridge, England, 1976.

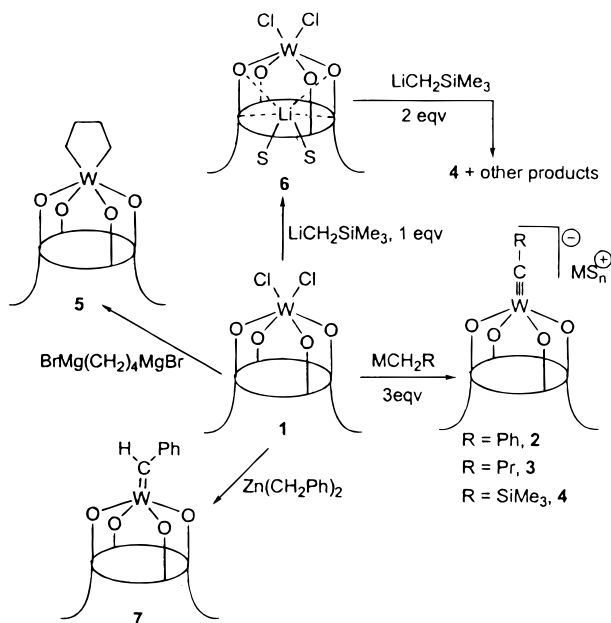
(16) Sheldrick, G. M. SHELXL93. Program for crystal structure refinement. University of Göttingen; Göttingen, Germany, 1993.

(17) See paragraph at the end of paper regarding Supporting Information.

Table 1. Experimental Data for the X-ray Diffraction Studies on Crystalline Complexes **2**, **4**, **7**, **9**, **13py**, **16**, and **19**

	2	4	7	9	13py	16	19
formula	C ₅₁ H ₅₇ O ₄ W· 0.5C ₃₀ H ₃₀ Mg· N ₆ ·2C ₅ H ₅ N	C ₆₀ H ₈₅ LiO ₇ SiW· C ₄ H ₈ O·C ₇ H ₈	C ₅₁ H ₅₈ O ₄ W· 2C ₄ H ₁₀ O	C ₄₉ H ₆₄ O ₄ SiW	C ₁₀₆ H ₁₂₈ Ag ₂ N ₂ O ₈ W ₂ · 2C ₃ H ₅ N·2C ₄ H ₁₀ O ₂	C ₁₃₀ H ₁₃₄ MgO ₁₀ W ₂ · 8C ₇ H ₈	C ₁₀₂ H ₁₁₄ O ₈ W ₂ · 3C ₆ H ₆ ·C ₅ H ₁₂
<i>a</i> , Å	22.038(3)	19.561(4)	12.978(2)	13.042(2)	12.661(2)	21.828(4)	14.867(1)
<i>b</i> , Å	12.415(2)	16.704(3)	18.977(4)	13.503(2)	24.283(3)	23.700(4)	16.100(1)
<i>c</i> , Å	25.171(3)	21.506(4)	21.858(4)	15.708(3)	19.461(3)	31.885(8)	25.700(2)
α, deg	90	90	90	66.42(2)	90	90	74.51(1)
β, deg	98.74(1)	107.06(2)	90	64.83(2)	105.71(2)	106.33(3)	76.74(1)
γ, deg	90	90	90	84.94(2)	90	90	73.97(1)
<i>V</i> , Å ³	6806.9(17)	6718(2)	5883.3(17)	2283.4(9)	5759.7(16)	15829(6)	5616.6(8)
<i>Z</i>	4	4	4	2	2	4	2
formula wt	1325.5	1301.4	1067.1	929.0	2480.1	2985.6	2142.2
space group	<i>P</i> 2 ₁ / <i>c</i> (No. 14)	<i>P</i> 2 ₁ / <i>c</i> (No. 14)	<i>P</i> na2 ₁ (No. 33)	<i>P</i> 1 (No. 2)	<i>P</i> 2 ₁ / <i>c</i> (No. 14)	<i>P</i> 2 ₁ / <i>c</i> (No. 14)	<i>P</i> 1 (No. 2)
<i>t</i> , °C	22	−130	22	−50	−130	22	22
λ, Å	0.710 69	0.710 69	0.710 69	0.710 69	0.710 69	0.710 69	0.710 69
ρ _{calc} , g cm ^{−3}	1.293	1.287	1.317	1.351	1.430	1.253	1.267
μ, cm ^{−1}	17.86	18.23	22.37	26.48	24.23	15.43	21.42
transmissn coeff	0.836–1.000	0.730–1.000	0.761–1.000	0.774–1.000	0.695–1.000	0.713–1.000	0.617–1.000
<i>R</i> ^a	0.054	0.039	0.046 [0.066] ^b	0.076	0.049	0.058	0.042
<i>wR</i> ₂	0.148	0.102	0.113 [0.185] ^b	0.235	0.126	0.156	0.104
GOF	1.067	1.017	1.060	1.150	1.013	1.061	1.160
<i>N</i> -observed ^c	7981	9170	9428	5335	8886	22 233	13 639
<i>N</i> -independent ^d	11 982	11 601	11 537	9246	11 883	31 201	15 216
<i>N</i> -refinement ^e	10 406	10 699	9428	8353	10 780	22 233	14 809
variables	745	727	589	492	644	1637	1113

^a Calculated on the observed reflections. ^b Values in brackets refer to the "inverted" structure. ^c *N*-observed is the total number of the independent reflections having $I > 2\sigma(I)$. ^d *N*-independent is the number of independent reflections. ^e *N*-refinement is the number of reflection used in the refinement having $I > 0$ for **2**, **4**, **9**, **13py**, and **19** and $I > 2\sigma(I)$ for **7**, and **16** and corrected for absorption.

Scheme 1

reaction path (α elimination vs reduction) and in the separation of magnesium and lithium halides. The best results were obtained at low temperature in toluene. The separation of salts was often a problem and not easy to explain: for example, a good yield of **2** was collected from THF, whereas Mg salts stayed in solution. The addition of DME helped the separation of LiCl and reduced the solubility of anionic complexes, probably breaking down dynamic aggregates of these complexes and their countercations.

Recent work by Schrock gave evidence of the possibility of obtaining $M\equiv C$ functionalities by loss of H_2 from W(IV) primary alkyls.¹⁸ This raises the question of the actual mechanism of the direct generation of alkyldynes described above, especially considering the fact that, using 1 or 2 equiv of

MCH₂R (M = Li, Mg; R = Ph, SiMe₃, Buⁿ), reduced, rather than alkylated, species were obtained. The reaction of **1** with LiCH₂SiMe₃ was studied in some detail: the 1:1 reaction in THF led cleanly to the W(V) lithium dichloride derivative **6**, which further reacted with 2 equiv of LiCH₂SiMe₃ in toluene to give only minor amounts of **4** (roughly 20–30%), the other main products appeared to be paramagnetic, their spectra being spread over 30 ppm), while the direct reaction of **1** with 3 equiv of LiCH₂SiMe₃ was almost quantitative, regardless of the solvent (NMR). When the 3:1 reaction was performed in Et₂O, no H₂ was produced, according to a GC analysis of the gas phase. This suggests that the process leading to alkylation is alternative to the reduction path.¹⁹ Using less reducing alkylating agents in a 2:1 ratio, dialkyls/alkylidenes could be prepared. Reacting **1** with butyl-1,4 di-Grignard in a 1:1 molar ratio, the dialkyl species **5** (best prepared by electron-transfer-catalyzed coupling of ethylene) was obtained, without the formation of any paramagnetic species. The reaction of **1** with Zn(CH₂Ph)₂ led to the phenyl alkyldiene **7**, first prepared by protonation of the corresponding alkyldyne **2** (see below).

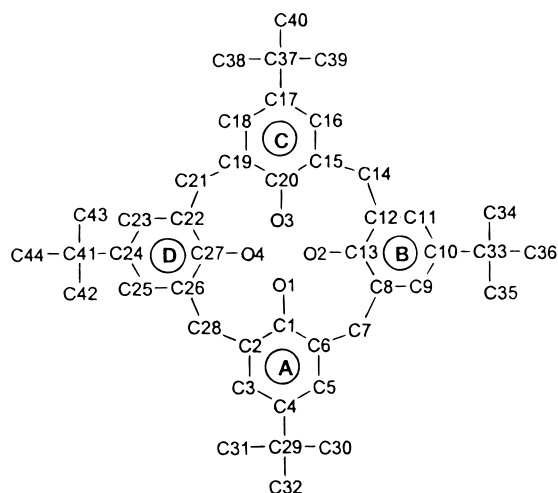
Complexes **2–4** were found to be thermally and photochemically very stable. Their NMR spectra in coordinating solvents showed a C_{4v} symmetric calix[4]arene moiety. The alkyldyne carbon gave a signal at 260–300 ppm in ¹³C NMR spectra. For complex **3**, a *J*_{CW} of 278 Hz was obtained, in agreement with literature data on alkyldynes.²⁰ Complexes **2** and **4** were characterized crystallographically. The labeling scheme adopted for the calix[4]arene–W moiety for all complexes is indicated in Chart 1. Selected bond distances and angles are quoted in Table 2 for complexes **2**, **4**, **7**, and **9** and in Table 3 for complexes **13py**, **16**, and **19**. In Table 4, a comparison of

(18) (a) Shih, K.-Y.; Totland, K.; Seidel, S. W.; Schrock, R. R. *J. Am. Chem. Soc.* **1994**, *116*, 12103. (b) Schrock, R. R.; Seidel, S. W.; Möschen-Zanetti, N.; Dobbs, D. A.; Shih, K.-Y.; Davis, W. M. *Organometallics* **1997**, *16*, 5195. (c) Schrock, R. R. *Acc. Chem. Res.* **1997**, *30*, 9.

(19) Schrock, R. R.; Clark, D. N.; Wengrovius, J. H.; Rocklage, S. M.; Pedersen, S. F. *Organometallics* **1982**, *1*, 1645 and references therein.

(20) Mayr, A.; Hoffmeister, H. *Adv. Organomet. Chem.* **1991**, *32*, 227.

Chart 1

**Table 2.** Selected Bond Distances (Å) and Angles (deg) for Complexes **2**, **4**, **7**, and **9**

	2	4	7	9
W(1)–O(1)	2.000(5)	2.026(2)	1.835(5)	1.857(10)
W(1)–O(2)	1.995(5)	1.969(3)	1.995(3)	1.969(7)
W(1)–O(3)	1.959(5)	1.944(3)	1.853(4)	1.864(11)
W(1)–O(4)	1.986(5)	1.963(3)	1.988(4)	1.972(9)
W(1)–C(45)	1.728(7)	1.759(4)	1.913(4)	1.914(10)
C(45)–C(46)	1.445(9)		1.437(6)	1.487(19)
Li–O(1)		1.908(10)		
Si–C(45)		1.835(4)		1.883(16)
W(1)–C(45)–C(46)	173.8(6)		135.2(4)	120.4(9)

relevant conformation parameters within the calix[4]arene–W unit is reported.

The structure of the pyridine solvate of **2** consists of the [*p*-Bu^t-calix[4]-(O)₄]W≡CPh][−] anion (Figure 1, Table 2) and the centrosymmetric cation [Mg(Py)₆]²⁺, with two additional molecules of pyridine, one of them hosted in the calix[4]arene cavity. Tungsten exhibits a square-pyramidal coordination involving the four oxygen atoms of calix[4]arene at the base and the C(45) carbon atom of the benzylidyne ligand at the apex. The W–C(45) bond length [1.722(7) Å] has a triple bond character.^{2,20} The direction of the W–C(45) bond forms a

dihedral angle of 1.9(3)° with the normal to the planar {O₄} core. Tungsten is displaced by 0.328(1) Å from this plane toward the C(45) carbon. The W–O bond distances, which are in a fairly narrow range, are slightly longer than those observed in neutral [*p*-Bu^t-calix[4]-(O)₄]W] derivatives containing WCl₂, W=O,^{11a} and W(OAr)₂²¹ functionalities. Calix[4]arene shows a cone conformation as is usually found in square-pyramidal five-coordinated metals. The almost symmetrical conformation is indicated by the narrow range of the dihedral angles formed by the plane through the C(7), C(14), C(21), C(28) bridging methylene carbons (*reference plane*) and the aromatic rings [119.5(2)–125.1(2)°]. The *reference plane* is parallel to the {O₄} core [dihedral angle 1.3(1)°].

Complex **4** was crystallized from THF/toluene, and its structure is depicted in Figure 2. The calix[4]arene ligand is in a cone conformation with greater distortion than in complex **2** (see Table 4), the {O₄} core is essentially planar; W is out of plane by 0.341(1) Å. The greatest difference with respect to the structure of **2** consists of the coordination of the Li⁺ cation to O(1). As a consequence of the steric bulk of the Li(thf)₃ group, the SiMe₃ group is bent by 30° with respect to the expected linear geometry. Apparently the geometrical distortion does not affect the triple bond nature of the W–C interaction, as shown by the W–C bond distance [1.720(7) Å]. In addition, the W–O(1) distance is only slightly affected by Li coordination (Table 2).

Reactions with Electrophiles: Generation of Alkylidenes.

The electron-rich, anionic alkylidyne species seemed to be particularly good candidates for reactions with electrophiles, summarized in Scheme 2.

The (reversible) protonation of **2**–**4** led cleanly to the corresponding alkylidenes (the trimethylsilyl derivative was not isolated, because of its very high solubility) without any other major change in the coordination sphere of the metal, as is usually the case when monodentate ligands are used. Although the protonation of alkylidynes is known, it is not reversible and occurs with important modifications in the coordination geometry and changes in the nature of the donor atoms around the metal.²² Many alkylidenes with β-hydrogens are believed to rearrange to olefins; carefully documented examples essentially do not exist, although much evidence points in that direction.²³ We observed that not only **7** but also **8**, which contains

Table 3. Selected Bond Distances (Å) and Angles (deg) for Complexes **13py**, **16**, and **19**

13py ^a		16		19	
W(1)–O(1)	1.872(5)	W(1)–O(1)	1.801(5)	W(1)–O(1)	1.848(5)
W(1)–O(2)	2.013(4)	W(1)–O(2)	2.101(4)	W(1)–O(2)	1.997(3)
W(1)–O(3)	1.951(5)	W(1)–O(3)	1.839(4)	W(1)–O(3)	1.838(4)
W(1)–O(4)	1.996(4)	W(1)–O(4)	1.950(4)	W(1)–O(4)	2.004(3)
W(1)–C(45)	1.832(5)	W(1)–C(45)	1.908(6)	W(1)–C(45)	2.089(6)
Ag(1)–N(1)	2.247(6)	Mg(1)–O(2)	2.002(4)	W(1)–C(46)	2.082(6)
Ag(1)–C(45)	2.312(6)	Mg(1)–O(5)	1.891(5)	C(45)–C(46)	1.439(8)
Ag(1)–C(45)′	2.562(6)	O(5)–C(46)	1.297(8)	C(45)–W(1)–C(46)	40.3(2)
C(45)–C(46)	1.492(8)	C(45)–C(46)	1.535(7)	W(1)A–C(45)–W(1)B	105.1(2)
O(1)–W(1)–O(3)	147.3(2)	C(46)–C(47)	1.352(8)	W(1)–C(45)–C(53)	132.1(4)
O(1)–W(1)–O(2)	86.1(2)	W(1)–C(45)–C(48)	122.8(4)	W(1)–C(45)–C(46)	69.6(3)
C(45)–Ag(1)–C(45)′	109.3(2)	W(1)–C(45)–C(46)	119.1(4)	C(46)–C(45)–C(53)	136.0(5)
N(1)–Ag(1)–C(45)′	121.0(2)	C(46)–C(45)–C(48)	117.1(5)	W(1)–C(46)–C(45)	70.1(3)
N(1)–Ag(1)–C(45)	129.6(2)			W(1)A–C(46)–W(1)B	105.6(2)
Ag(1)–C(45)–Ag(1)′	70.7(2)			C(45)–C(46)–C(47)	135.1(5)
W(1)–C(45)–Ag(1)′	94.5(2)			W(1)–C(46)–C(47)	120.5(4)
W(1)–C(45)–Ag(1)	97.6(2)				
Ag(1)′–C(45)–C(46)	108.4(4)				
Ag(1)–C(45)–C(46)	113.3(4)				
W(1)–C(45)–C(46)	146.0(4)				

^a A prime denotes a transformation of 1 – x, –y, and 1 – z.

Table 4. Comparison of Relevant Conformational Parameters within Calix[4]arene for Complexes **2**, **4**, **7**, **9**, **13py**, **16**, and **19**

	2	4	7	9	13py	16	19
(a) Distance (Å) of Atoms from the O ₄ Mean Plane							
O(1)	-0.013(5)	0.021(4)	-0.124(4)	-0.079(7)	-0.143(4)	-0.158(4)	-0.137(5)
O(2)	0.014(5)	-0.021(4)	0.087(3)	0.107(9)	0.130(4)	0.153(4)	0.128(5)
O(3)	-0.014(5)	0.022(4)	-0.117(4)	-0.104(9)	-0.122(4)	-0.152(4)	-0.142(5)
O(4)	0.014(5)	-0.021(4)	0.119(4)	0.080(8)	0.127(4)	0.156(4)	0.127(5)
W	0.331(1)	0.341(1)	0.368(1)	0.384(1)	0.404(1)	0.357(2)	0.454(1)
(b) Dihedral Angles (deg) between Planar Moieties ^a							
E∧A	124.6(1)	114.8(1)	137.2(1)	136.1(3)	142.4(1)	142.0(2)	130.7(1)
E∧B	122.1(2)	126.6(1)	114.1(1)	126.0(4)	118.5(1)	111.9(1)	116.9(1)
E∧C	125.2(2)	125.3(1)	131.8(1)	128.5(3)	128.2(1)	136.2(2)	137.7(1)
E∧D	119.5(2)	130.9(1)	116.3(1)	120.7(3)	111.8(1)	113.8(2)	117.2(2)
A∧C	110.2(2)	120.0(1)	90.9(2)	95.4(4)	90.6(2)	98.3(2)	91.6(2)
B∧D	118.4(2)	102.4(1)	129.6(2)	113.2(4)	129.7(2)	134.3(2)	126.8(2)
(c) Contact Distances (Å) between Para Carbon Atoms of Opposite Aromatic Rings							
C(4)⋯C(17)	8.485(11)	7.953(7)	9.268(8)	9.05(2)	9.346(7)	9.614(9)	9.232(11)
C(10)⋯C(24)	8.038(10)	8.847(7)	7.411(9)	8.269(17)	7.428(10)	7.208(10)	7.542(8)

^a E (reference plane) refers to the least-squares mean plane defined by the C(7), C(14), and C(21), C(28) bridging methylenic carbons.

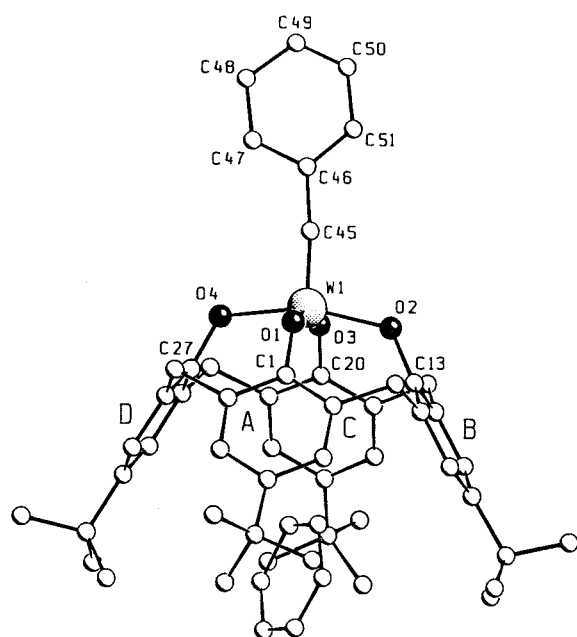


Figure 1. SCHAKAL view of the anion in complex **2**. Disorder affecting the pyridine guest molecule has been omitted for clarity.

β -hydrogens, were thermally and photochemically highly stable.¹⁸ In the ¹H NMR spectra, the calix[4]arene moiety appeared to be of C_{4v} symmetry: like the related η^2 -alkene/alkyne species, the carbene ligand must have a very small rotational barrier (see extended Hückel Analysis). The signal of W=C(H)R was found at ~10 ppm. It is of interest to notice that, in the case of **8**, when pyridine was used as solvent, the coupling of the alkylidene H to its carbon as well as to the adjacent CH₂ was lost: we interpret this in terms of a rapid reversible deprotonation of the former by the basic solvent. In the ¹³C NMR spectrum of **8** in C₆D₆, the carbon bound to tungsten atom gave

(21) Zanotti-Gerosa, A.; Solari, E.; Giannini, L.; Floriani, C.; Chiesi-Villa, A.; Rizzoli, C. *J. Chem. Soc., Chem. Commun.* **1996**, 119.

(22) (a) Reference 2, Chapter 4. (b) Reference 2, Chapter 5. (c) Clark, G. R.; Marsden, K.; Roper, W. R.; Wright, L. J. *J. Am. Chem. Soc.* **1980**, *102*, 6570. (d) Weber, L.; Dembeck, G.; Stammeler, H.-G.; Neumann, B.; Schmidtman, M.; Müller, A. *Organometallics* **1998**, *17*, 5254. (e) Kim, H. P.; Kim, S.; Jacobson, R. A.; Angelici, R. J. *Organometallics* **1984**, *3*, 1124. (f) Doyle, R. A.; Angelici, R. J. *Organometallics* **1989**, *8*, 2207. (g) Green, M.; Orpen, A. G.; Williams, I. D. *J. Chem. Soc., Chem. Commun.* **1982**, 493.

(23) (a) Freudenberg, J. H.; Schrock, R. R. *Organometallics* **1985**, *4*, 1937. (b) Hatton, W. G.; Gladysz, J. A. *J. Am. Chem. Soc.* **1983**, *105*, 6157.

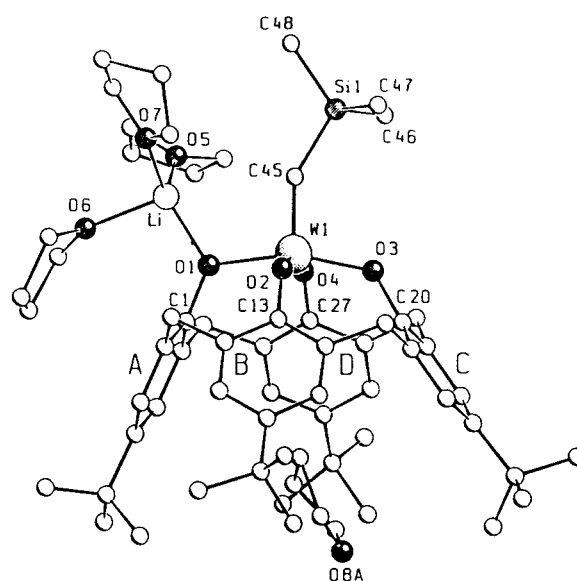


Figure 2. SCHAKAL view of complex **4**. Disorder affecting the butyl groups associated with the C and D rings and the THF guest molecule have been omitted for clarity.

a signal at 272 ppm, very close to that of the corresponding alkylidene; the more diagnostic J_{CW} was much lower than for **3**, only 180 Hz.^{6,24} The value of J_{CH} , 142 Hz, rules out any agostic coordination of the α hydrogen to W.⁶

Complex **7** was structurally characterized (Figure 3). According to the structural parameters in Tables 2 and 4, the coordination polyhedron is a trigonal elongated bipyramid involving the O(1), O(3), and C(45) atoms in the equatorial plane and the O(2) and O(4) atoms at the axial positions. The W–C(45) bond length [1.913(4) Å], remarkably longer than the corresponding ones in **2** and **4**, is consistent with a metal–carbon double bond.^{1,6} W–O bond lengths are alternate, with the mean value of the W–O(1) and W–O(3) distances [1.846(9) Å] significantly shorter than the mean value of the W–O(2) and W–O(4) distances [1.992(3) Å]. The phenyl-alkylidene ligand is oriented nearly perpendicular to the O₄ core in such a way as to point the H(51) ortho hydrogen atom toward the O(1) oxygen atom, giving rise to a puckered six-membered chelation ring through an intramolecular interaction consistent with a C–H⋯O hydrogen bond: C(51)⋯O(1), 3.288(7) Å;

(24) Köhler, F. H.; Kalder, H. J.; Fischer, E. O. *J. Organomet. Chem.* **1976**, *113*, 11.

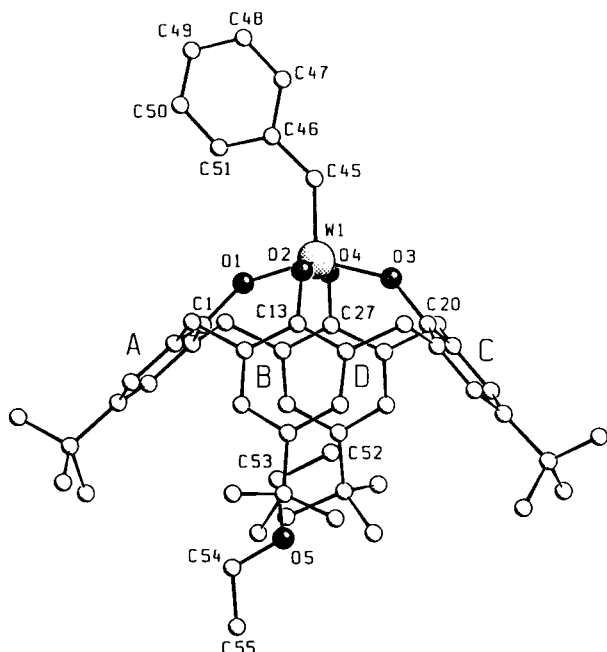
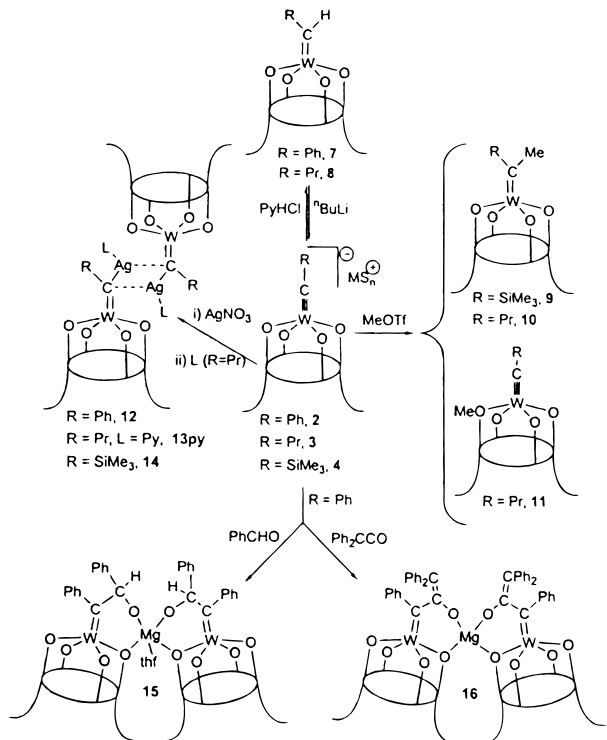


Figure 3. A SCHAKAL view of complex **7**. Disorder affecting the butyl groups associated with the A and B rings has been omitted for clarity.

Scheme 2



H(51)···O(1), 2.59 Å; C(51)–H(51)···O(1), 132.6°. The calix[4]arene unit assumes an elliptical cone section (see Table 4), W protruding out of the O₄ plane by 0.359(1) Å.

The reaction of **4** with MeOTf, known to be a powerful source of Me⁺, led to the isolation of the alkylidene **9** (Scheme 2), which was fully characterized, including a crystal structure shown in Figure 4.

The coordination polyhedron is a trigonal elongated bipyramid involving the O(1), O(3), and C(45) atoms in the equatorial plane and the O(2) and O(4) atoms at the axial positions. The main structural features are similar to those observed in **7**: (i) the O₄

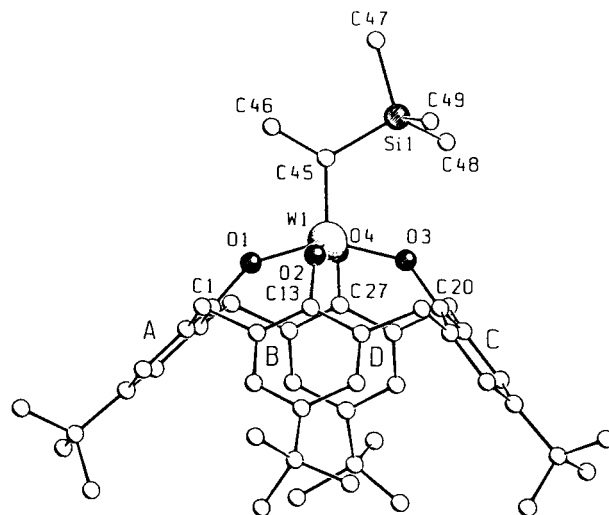


Figure 4. SCHAKAL view of complex **9**. Disorder affecting the butyl groups associated with the B and D rings has been omitted for clarity.

core shows significant tetrahedral distortions with tungsten displaced by 0.384(1) Å toward the C(45) atom (Table 4); (ii) the four W–O bond lengths are different, the mean value of the W–O(1) and W–O(3) distances [1.861(11) Å] being significantly shorter than the mean value of the W–O(2) and W–O(4) distances [1.971(8) Å]; (iii) the W–C(45) [1.914(10) Å] bond length is close to that in **7** (Table 2).

The reaction with MeOTf was not as clean as that with PyHCl: another product of lower symmetry was detected by ¹H NMR in the reaction mixture. Performing the same alkylation reaction on **2** or **3** we obtained mixtures of two products, in similar amounts, of apparent C_{4v} and of C_s symmetry (NMR). The regiochemistry of the alkylation with MeOTf seems to depend mainly on the alkylidene: the ratio of the two products was almost the same performing the reaction at room temperature or at –80 °C. The mixture of the two products **10** and **11** obtained in the alkylation of **3** was characterized by NMR methods. **10** is the analogue of **9**. The alkylidene carbon fell at 293 ppm, with a J_{CW} of 177 Hz, while the methyl group gave a signal at 28.4 ppm in ¹³C NMR and at 5.52 ppm in ¹H NMR; the latter exhibited cross-peaks with signals from the Pr residue in a TOCSY (¹H–¹H) experiment.²⁵ Complex **11** showed a C_s symmetry, with three signals for the Bu^t (2:1:1) and two pairs of doublets for the bridging methylenes in ¹H NMR. The alkylidene carbon fell at 301.7 ppm, with a J_{CW} of 278 Hz, while the methoxy group gave a signal at 80.7 ppm in ¹³C NMR and at 5.12 ppm in ¹H NMR; the latter did not show any cross-peak with signals from the Prⁿ residue in a TOCSY (¹H–¹H) experiment.²⁵

A synthetically useful derivatization of the anionic alkylidynes **2–4** would be their metalation, which, in the present case, was performed using the carbophilic Ag⁺. A different kind of M≡C metalation reaction leading to dimetallacyclopropenes, rather than to the class of compounds here mentioned, has been reported.²⁶ Complexes **2–4** reacted with AgNO₃ to give **12–14** (Scheme 2). Elemental analysis first indicated the successful exchange of Li⁺ or Mg²⁺ with Ag⁺. The ¹H NMR of the three species was similar to those of the respective starting materials,

(25) Braun, S.; Kalinowski, H.-O.; Berger, S. *100 and More Basic NMR Experiments, a Practical Course*; VCH: Weinheim, Germany, 1996.

(26) (a) Clark, G. R.; Cochrane, C. M.; Roper, W. R.; Wright, L. J. *J. Organomet. Chem.* **1980**, *199*, C35. (b) Stone, F. G. A. *Angew. Chem., Int. Ed. Engl.* **1984**, *23*, 89.

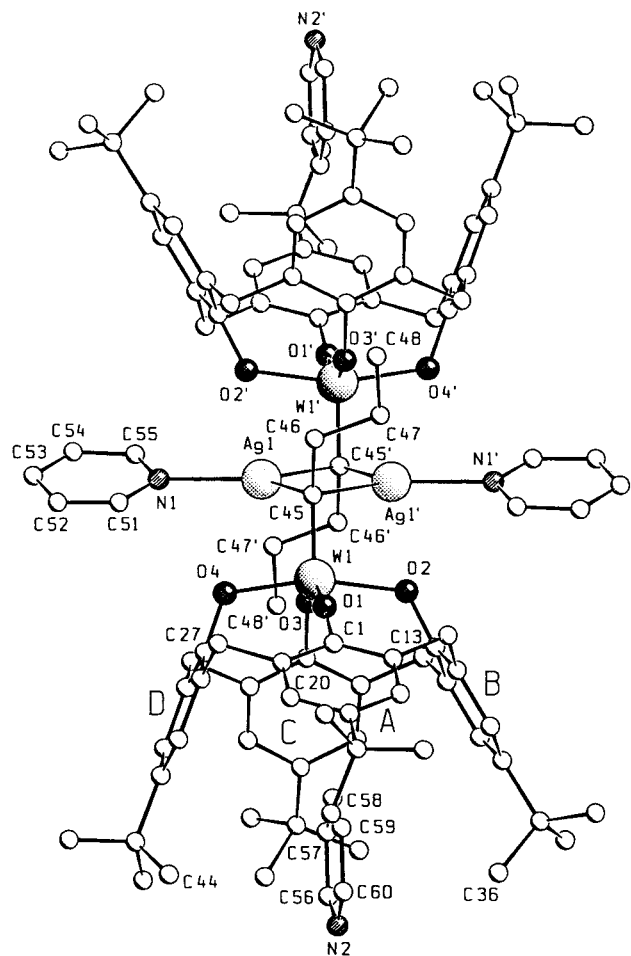


Figure 5. SCHAKAL view of complex **13py**. Disorder affecting the butyl groups associated with the A and C rings has been omitted for clarity. Prime denotes a transformation of $1 - x, -y, 1 - z$.

hence not very informative. Complex **12** was by far the most soluble of the three, so most of the spectroscopic work was done on it.

The ^{13}C NMR spectrum of **12** in noncoordinating solvents showed a broad triplet at 241 ppm, which was attributed to the coupling of the alkylidene carbon with two equivalent (on the NMR time scale) Ag^+ ions ($J_{\text{Cag}} = 59\text{--}60$ Hz). As a consequence, in solution the product must be at least a dimer, but most likely a tetramer, given the preference of Ag^+ for linear coordination.²⁷

X-ray analysis of the pyridine solvate **13py** showed the latter to be a dimer (Figure 5), where two silver ions bridge two alkylidene fragments and are further coordinated by a pyridine molecule. Planar trigonal coordination has commonly been encountered in Cu^+ and Ag^+ alkyl/aryl species in the presence of N-donors.²⁷

Complex **13py** crystallizes as a centrosymmetric dimer, hosting a pyridine molecule in each aromatic cavity. The calix[4]arene assumes an elliptical cone conformation, W protruding of 0.404(1) Å from the $\{\text{O}_4\}$ core (maximum deviation from planarity 0.18 Å) (Table 4). The W–O bond distances fall within the range of values observed for the present compounds (Table 3), the shortest distance [W–O(1), 1.872(5) Å] corresponding to the largest bond angle [W–O(1)–C(1), 162.2(4)°]. The polyhedron coordination could be described as a trigonal

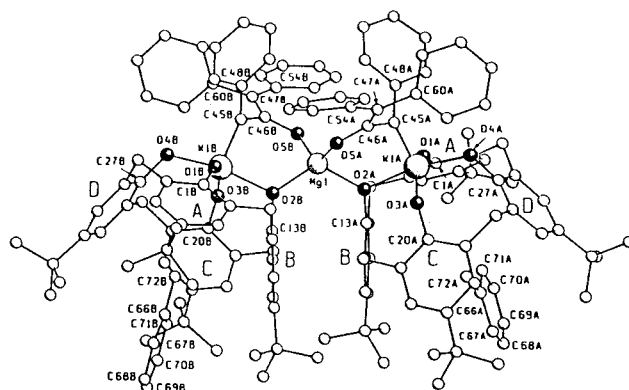


Figure 6. SCHAKAL view of complex **16**. Disorder affecting the butyl groups associated with the C ring (molecule A) and the A and C rings (molecule B) has been omitted for clarity.

elongated bipyramid involving the O(1), O(3), and C(45) atoms in the equatorial plane and the O(2) and O(4) atoms at the axial positions. The W–C distance is 1.832(5) Å, and the angle W(1)–C(51)–C(52) is 145.83(56)°. These parameters are close to those corresponding to an alkylidene, as expected given the high carbophilicity of Ag^+ . The silver cations behave as asymmetric bridges [W–C(45), 2.312(6) Å vs W–C(45'), 2.562(6) Å]. The resulting Ag_2C_2 inner core, which is planar from symmetry requirements, is sandwiched between parallel O_4 cores [dihedral angle $\text{Ag}_2\text{C}_2\wedge\text{O}_4$, 8.0(1)°]. The silver cation achieves a trigonal coordination through the N1 nitrogen atom from a pyridine molecule.

The mode of Ag^+ coordination, and hence the nature of the complex can be modified by added ligands. The silver derivatives did not seem to retain an aggregated structure in neat pyridine: both **12** and **13** exhibited a singlet at 265–270 ppm in their ^{13}C NMR in $\text{Py-}d_5$. In the case of **12**, J_{CW} was determined: its value, 256 Hz, is typical of alkylidene species.^{20,24} It should be noted that the color changed from red to yellow when **12** was dissolved in pyridine (the parent alkylidene **2** is yellow, the parent alkylidene **7** brown).

Alkylidynes can also react with neutral electrophiles, such as a carbonyl functionality, provided it is sterically accessible. The reaction between **2** and benzaldehyde (Scheme 2) illustrates the possibility of using anionic alkylidynes as organometallic Grignard reagents. **15** has a rigid structure, as shown by the lack of symmetry in NMR, even in $\text{Py-}d_5$ (where in any case THF is exchanged). The alkylidene carbon falls at 291 ppm; the former carbonyl carbon of the benzaldehyde moiety gives a signal at 79.3 ppm and is bound to the H giving the singlet at 10.2 ppm in ^1H NMR (HSQC).²⁵ The proposed structure of **15** (Scheme 2) is also supported by the crystal structure of **16**, obtained in an analogous reaction of **2** with diphenylketene. Possibly because of the steric demand of the CPh_2 group, **16** is rather fluxional in solution, and a good ^1H NMR, indicating the C_s symmetry of the complex, could only be obtained at low temperature (253 K).

The structure of **16** consists of two crystallographically independent anions (called A and B) bridged by a magnesium cation (Figure 6). Magnesium is tetrahedrally coordinated to the calix[4]arene O(2) oxygen atoms and the O(5) enolato oxygen atoms from the two anions. The two independent anions have similar geometry. Thereafter the values refer to the anion A. Values for molecule B are given in Supporting Information. The O_4 core is tetrahedrally distorted with tungsten protruding by 0.357(2) Å from the mean plane toward the C(45) atom (Table 4). The trend of bond distances and angles in the

(27) Van Koten, G.; James, S. L.; Jastrzebski, B. H. In *Comprehensive Organometallic Chemistry II*; Abel, E. W., Stone, F. G. A., Wilkinson, G., Eds.; Pergamon: Oxford, U.K., 1995; Vol. 3; Chapter 2.

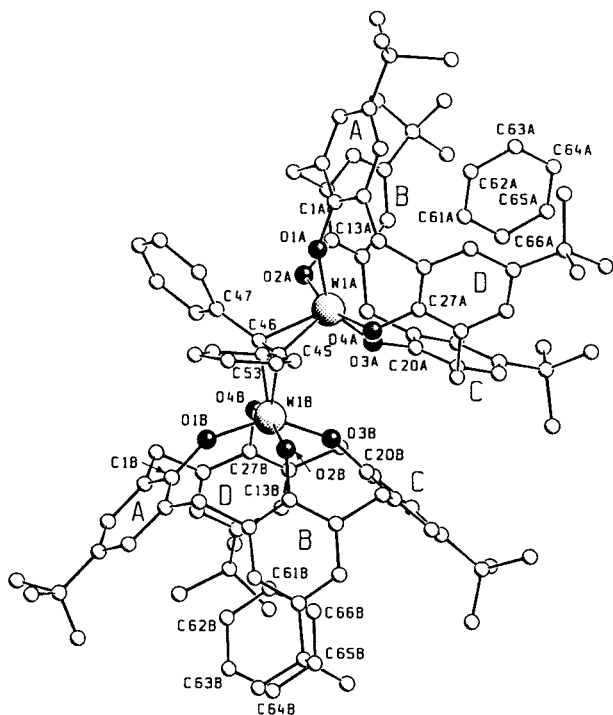
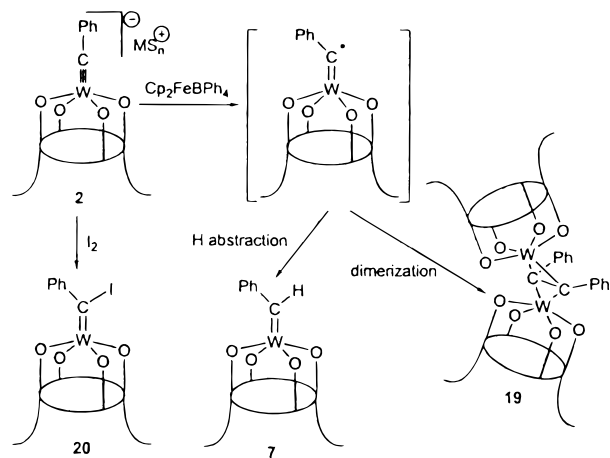


Figure 7. SCHAKAL view of complex **19**. Disorder affecting the butyl groups associated with the A, B, and C rings (molecule A) and the A ring (mol B) has been omitted for clarity.

Scheme 4



C(45)–C(46) [1.439(8) Å] suggest a bismetallacyclopropane structure. The two independent $[\{p\text{-Bu}^t\text{-calix[4]-(O)}_4\}\text{W}]$ moieties show a very close geometry. Thereafter, the values refer to the fragment A. Values for molecule B are reported in Supporting Information. The O_4 core is tetrahedrally distorted with tungsten protruding by 0.454(1) Å from the mean plane toward the $\mu\text{-C}_2$ bridge. The W, C(45), and C(46) plane is perpendicular to the O_4 mean plane, the dihedral angle between them being 95.2(2)°. The trend of bond distances and angles in the coordination sphere (Table 3) is similar to that observed in **7**, **9**, and **16** (Tables 2 and 3). So the coordination polyhedron could be described as an elongated trigonal bipyramid having the O(1), O(3), and C(45) atoms in the equatorial plane and the O(2) and O(4) atoms at the axial positions, with the calix[4]-arene unit having an elliptical cone conformation (Table 4).

The oxidation of complex **2** (Scheme 4), performed with I_2 , led to the clean isolation of halogen-substituted alkyldiene **20**,³² which exhibited a characteristic^{1,6} signal in ^{13}C NMR at 230

ppm with a coupling constant to ^{183}W of 212 Hz. The structure sketched in Scheme 4 is supported by a preliminary X-ray analysis.

Discussion

Chemical Considerations. In the basis of the synthetic sequence ending to the anionic W-alkylidynes, we are not able to discriminate between the two major mechanisms, namely, between the reductive alkylation followed by the alkylation of the reduced species with loss of H_2 , and a stepwise α -elimination. Although some data are in favor of the latter, both could occur simultaneously. The observed dependency of the alkylation pathway on the nature of the alkylating agent (Zn vs Mg and Li) and on the reaction solvents clearly indicates that both factors can affect more or less the carbanionic nature and by consequence the reducing properties of the reagent. However, regardless of the alkylation pathways, the reactions in Scheme 1 show how the preorganized $[\text{O}_4]^{4-}$ ligand preferentially drives the formation of W–C multiple bonds as compared with the simple W–alkyls. This fact is the consequence, as in Schrock's triamidoamine ligands,^{18c} of the appropriate set of frontier orbitals at the metal ready to form a σ - and two π -bonds.

However, the $[\text{O}_4]^{4-}$ ligand clearly has introduced two novelties in metal–alkylidyne chemistry: (i) the formation of anionic species; (ii) the assistance of the oxygen donor atoms in driving the alkyldiene reactivity. The alkyldiene derivatives **2–4** have two potential basic sites which can be engaged in the reaction with protons or, in general, with electrophiles (Scheme 2): the alkyldiene carbon and the oxygens from the calix[4]arene moiety. Protonation occurs selectively on carbon (Scheme 2), while the alkylation, depending on the alkyl substituent, does not discriminate very much and, eventually, both kinds of compound (see complexes **9** and **11** in Scheme 2) can be obtained. We do not know which one of the controlling factors, the charge or the frontier orbital set, is prevailing in either reaction (see below). However, we believe that both protonation and alkylation may involve the assistance of the oxygen. In support of this hypothesis, a significant structural feature of **7** should be emphasized, namely, the interaction of the proton from the alkyldiene carbon interacting with one of the calix[4]arene oxygens.

In addition, we should mention that the possibility of interconverting alkyldiene–alkylidene by protonation–deprotonation is due to the very high stability of the macrocyclic structure of the $[\text{O}_4]^{4-}$ unit. In all cases so far reported, such a reaction affects the ancillary ligands, with considerable changes in the coordination sphere of the metal.²²

The extension of the reaction to electrophiles other than H^+ and R^+ may be considered a synthetic methodology to otherwise inaccessible functionalized metal–alkylidenes. In the specific case of the reaction with PhCHO and $\text{Ph}_2\text{C}=\text{C}=\text{O}$, the regiochemistry (see complexes **15** and **16** in Scheme 2) is controlled, among other factors, by the oxophilicity of the counteraction Mg^{2+} , which has a particular preference for the alkoxo and enolato ligands. A remarkable access to functionalized alkyldiene complexes^{22c–f} comes from the oxidation of anionic alkyldynes with I_2 leading to the iodo–alkylidene **20** (Scheme 4).³² The iodo derivative could undergo substitution reactions with nucleophiles, thus introducing heteroatoms in the alkyldiene

(32) For haloalkylidene complexes, see: (a) Reference 19c. (b) Huang, D.; Caulton, K. G. *J. Am. Chem. Soc.* **1997**, *119*, 3185. (c) Brothers, P. J.; Roper, W. R. *Chem. Rev.* **1988**, *88*, 1293. (d) Morrison, J. A. *Adv. Organomet. Chem.* **1993**, *35*, 211. (e) Doherty, N. M.; Hoffman, N. W. *Chem. Rev.* **1991**, *91*, 553. (f) Mansuy, D.; Lange, M.; Chottard, J. C.; Bartoli, J. F.; Chevrie, B.; Weiss, R. *Angew. Chem.* **1978**, *90*, 828.

backbone. While the former strategy serves more to introduce functionalities into the β -position, the latter one could be employed to introduce functionalities into the α -position of the alkylidene. $[[p\text{-Bu}^t\text{-calix[4]}-(\text{O})_4]\text{W-alkylidenes}]$ **7** and **8** display a quite low reactivity, exemplified by the formation of an adduct with benzaldehyde, which does not easily undergo a metathesis reaction. A quite unusual labilization of the $\text{W}=\text{C}$ double bond can however be achieved in the reaction with $\text{Bu}^t\text{-NC}$, leading to the loss of the carbene fragment (see Scheme 3, **17** and **18**). Such a kind of induced and nonspontaneous labilization could be particularly useful if it was necessary to keep the functionality stable in the presence of a substrate and then subsequently to induce its reactivity. The labilization reaction could make it possible to transfer functionalized alkylidenes to appropriate organic substrates.

A reaction that is strictly related to the anionic nature of the reported alkylidynes is the one-electron oxidation, leading to the free-radical species shown in Scheme 4. The free radical can be intercepted by the solvent via a hydrogen transfer or dimerizes to **19**. The latter event is particularly interesting since it suggests, in the case of success of the reverse reaction, the synthesis of alkylidynes and alkylidenes from acetylenes, and, better, the access to metal-carbido derivatives.

Extended Hückel Analysis. Extended Hückel calculations³³ were performed to elucidate the electronic structure of the $[[p\text{-Bu}^t\text{-calix[4]}-(\text{O})_4]\text{W-alkylidynes}]$, their reaction pathway with protons and electrophiles, and some aspects of their redox chemistry. The calix[4]arene ligands have been slightly simplified by replacing the Bu^t groups and the methylene bridges by hydrogens and symmetrizing to a C_{4v} or C_{2v} local symmetry. This simplified model retains the main features of the whole ligand; in particular, the geometrical constraints on the O_4 set of donors atoms is maintained by fixing the geometry of the four phenoxo groups to the experimental X-ray structural parameters.

The electronic structure of the alkylidyne compounds **2-4** and the alkylidene compounds **7** and **8** has been analyzed using as model complexes $[(\text{calix})\text{W}\equiv\text{CMe}]^-$ and $[(\text{calix})\text{W}=\text{C}(\text{H})\text{Me}]$, respectively.³⁴

The frontier orbitals of the $[\text{W}(\text{calix})]$ fragment consist of four low-lying metal d orbitals, as shown on the left in Figure 8. For a symmetrical C_{4v} geometry, the lowest energy metal orbital is a $1a_1(d_{z^2})$, with the degenerate $1e(d_{xz}, d_{yz}) \sim 0.5$ eV above. Due to the π -interactions with the oxygen atoms, the $1a_2(d_{xy})$ orbital lies 1.0 eV higher in energy. The $d_{x^2-y^2}$, pointing more closely toward the oxygen ligands, are pushed high in energy.

Figure 8 illustrates the expected bonding interactions of the $[\text{W}(\text{calix})]$ fragment with the CMe moiety,^{34a} i.e., between the $1a_1(d_{z^2})$ and the σ -donor $1a_1$ of CMe and between the two metal degenerate orbitals of the $1e$ set (d_{xz}, d_{yz}) and those of the π -acceptor $1e$ set (p_x, p_y).

These electron-rich anionic alkylidynes easily undergo reactions with electrophiles. The regiochemistry of the electrophilic attack may be determined by both charge and frontier orbital factors, and charge effects are expected to be important for these anionic alkylidyne species, especially when hard electrophiles such as H^+ or Me^+ are considered.³⁵ The results of the Mulliken

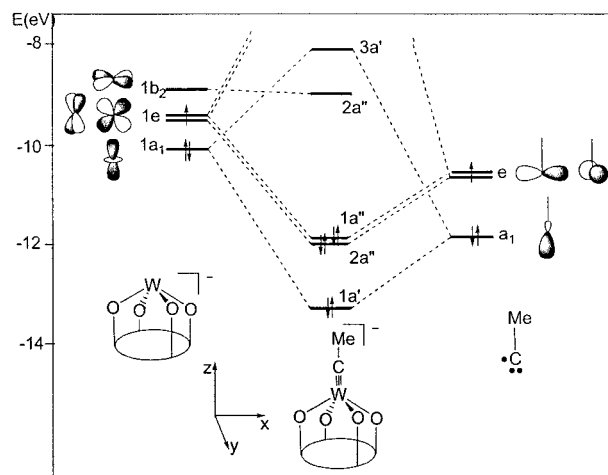


Figure 8. Molecular orbital interaction diagram for $[(\text{calix})\text{W}\equiv\text{CMe}]^-$.

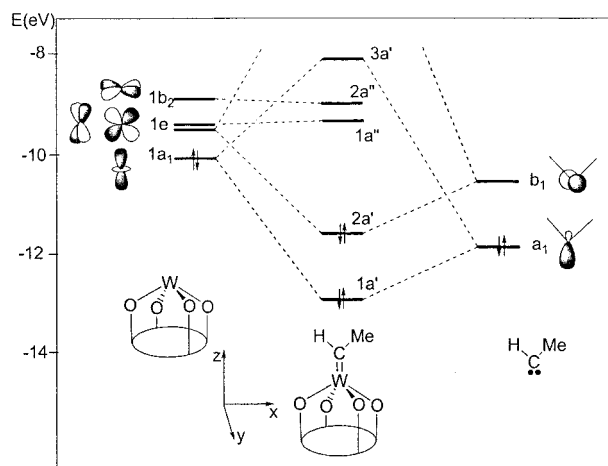


Figure 9. Molecular orbital interaction diagram for $[(\text{calix})\text{W}=\text{C}(\text{H})\text{Me}]$.

population analysis on $[(\text{calix})\text{W}\equiv\text{CMe}]^-$ show that the oxygen atoms and the alkylidyne carbon have by far the highest negative charges with almost equal values (-0.99 and -0.97) so that the incoming electrophiles are expected to attack both oxygen and carbon. This hypothesis agrees well with the regiochemistry experimentally observed for Me^+ attack, as the reaction of **2-4** with MeOTf leads to a mixture of both alkylidenes (resulting from C-attack) and O-methylated alkylidynes (resulting from O-attack). The protonation of **2-4** with PyHCl leads exclusively to alkylidenes, but this result could be due to the high mobility of the proton which may migrate easily from the oxygen to the carbon atom giving the most stable products. On the other hand, when a soft electrophile such as Ag^+ is considered, frontier orbital factors are expected to prevail,³⁵ so that the regiochemistry is determined by the high-lying HOMO, which has a $\text{W}-\text{C}$ π -character, more localized on the carbon atom. The regiochemistry observed for the reaction of **2-4** with AgNO_3 in fact leads to the silver-alkylidene species **12-14**.

Figure 9 illustrates the bonding interactions in the $[(\text{calix})\text{W}=\text{C}(\text{H})\text{Me}]$ alkylidene.^{34b} At variance with the alkylidyne, the π -interaction with the $\text{C}(\text{H})\text{Me}$ moiety engages only one of the two d_{π} orbitals, d_{yz} , which is no longer available to the π -donation from the calix[4]arene oxygens, thus $\text{W}-\text{O}$ bonds are single in the yz plane (perpendicular to the alkylidene unit). On the other hand, the π -donation from the oxygens in the xz plane to the d_{xz} metal orbital confers to $\text{W}-\text{O}$ bonds in the latter plane double bond character, thus explaining the strong C_{2v}

(33) (a) Hoffmann, R.; Lipscomb, W. N. *J. Chem. Phys.* **1962**, *36*, 2179. (b) Hoffmann, R. *J. Chem. Phys.* **1963**, *39*, 1397.

(34) For analogous MO calculations on $\text{M}=\text{C}$ and $\text{M}\equiv\text{C}$ bonds, see: (a) Reference 2, Chapter 3. (b) Dötz, K. H.; Fischer, H.; Hofmann, P.; Kreissl, F. R.; Schubert, U.; Weiss, K. *Transition Metal Carbene Complexes*; VCH: Weinheim, Germany, 1988; Chapter 4; pp 113-149.

(35) Fleming, I. *Frontier Orbitals and Organic Chemical Reactions*, Wiley: London, U.K.; 1976.

distortion of the [W(calix)] unit observed in the X-ray structure of **7** and **9**.

It is also worth noting that, in the [W(calix)] fragment, the presence of two orthogonal d_{π} orbitals, equally available for interaction with the π -system of the C(H)Me organic fragment, suggests a small activation barrier for the alkylidene rotation around the z -axis. Extended Hückel calculations with the organic fragment rotated by 45° with respect to the xz plane gave an estimated energy barrier of 3 kcal mol $^{-1}$. The expected free rotation of the alkylidene is supported by the ^1H NMR of **7** and **8**, indicating an apparent C_{4v} symmetry of the calix[4]arene moiety.

The coordination of the H–N \equiv C trans to the alkylidene unit leads to a strong destabilization of the d_z^2 orbital (interacting with the carbon lone pair of CNH) and a significant stabilization of the two d_{xz} d_{yz} orbitals (due to their interactions with the empty π^* -orbitals of CNH). Both effects lead to a higher energy mismatch between these metal orbitals and the interacting counterparts on the alkylidene unit and thus to a labilization of the metal–alkylidene bonding.

We finally considered the one-electron oxidation of the alkylidyne **2** and the corresponding C–C coupled species **19**. The orbital diagram of the methyl alkylidyne reported in Figure 8 shows that the HOMO is the doubly degenerate $1e$ orbital, describing the tungsten–carbon π -bonding, which is mainly localized on the carbon atom. The one-electron oxidation of these alkylidynes species leads therefore to carbon-centered radicals, in agreement with the experimentally observed coupling to the C–C bonded compound **19**.

Conclusions

The calix[4]arene macrocyclic tetraanion provides a unique chemical environment for tungsten involved in organometallic

chemistry. We should emphasize the consequences on the chemical reactivity of the metal center. The metal frontier orbitals in such an environment are particularly appropriate for stabilizing M–C multiple bonds and, particularly, the alkylidyne functionality.^{18c} Due to the tetraanionic nature and the macrocyclic stability of the ancillary ligand, some unique chemistry has been developed on the anionic alkylidynes: (i) the interconversion to the corresponding alkylidenes obtained via the reversible protonation–deprotonation reaction. Such a reaction may have the assistance of the basic oxygens of the coordination environment, as with the heterogeneous catalysts; (ii) the introduction of a variety of functional groups at the alkylidene carbon via the reaction with electrophiles, which is a novel synthetic methodology for obtaining unprecedented alkylidenes containing functional groups; (iii) the metalation leading to the formation of dimetallic alkylidenes; (iv) the one-electron oxidation leading to the oxidative coupling of the alkylidyne functionalities to the corresponding bridging acetylenes.

Acknowledgment. We thank the “Fonds National Suisse de la Recherche Scientifique” (Bern, Switzerland, Grant 20-53336.98), Ciba Specialty Chemicals Inc. (Basle, Switzerland), and Fondation Herbette (N.R.) for financial support.

Supporting Information Available: Details of the X-ray data collection, structure solution, and refinement; ORTEP or SCHAKAL drawings, tables giving crystal data, fractional atomic coordinates, anisotropic and isotropic thermal parameters, bond lengths, and bond angles for complexes **2**, **4**, **7**, **9**, **13py**, **16**, and **19** (PDF). Supporting Information is available free of charge via the Internet at <http://pubs.acs.org>.

JA9839015